

Automatic search for failed eruptions in SDO/AIA observations.

T.Mrozek, D. Gronkiewicz

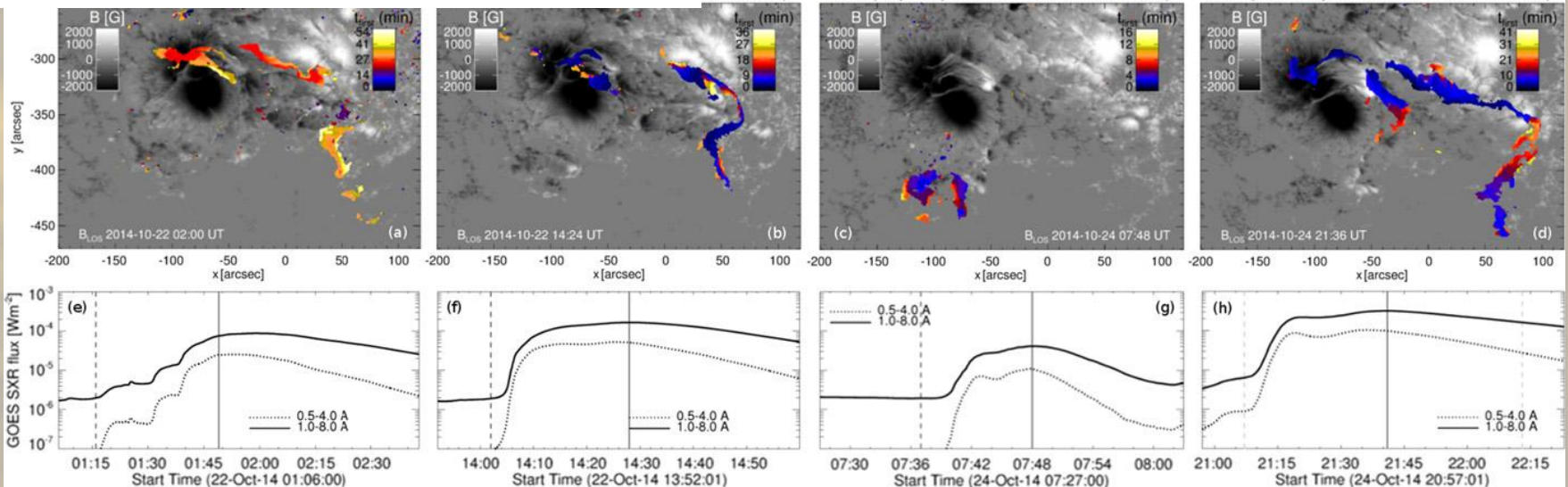
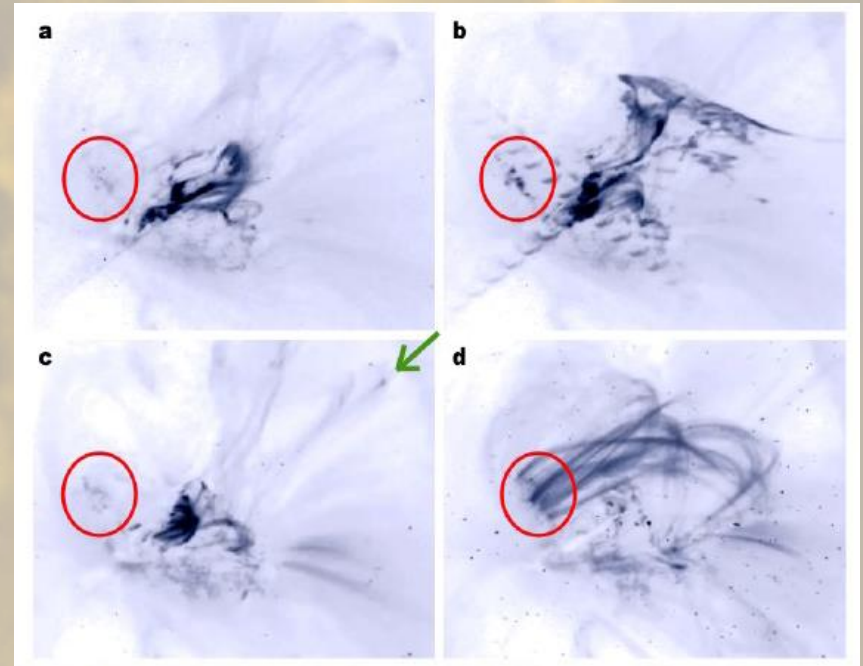
Why failed eruptions?

- Space weather
- Interaction between magnetic structures
- Particle acceleration in interaction region
- Stellar CMEs

AR12192, flare-rich and CME-poor

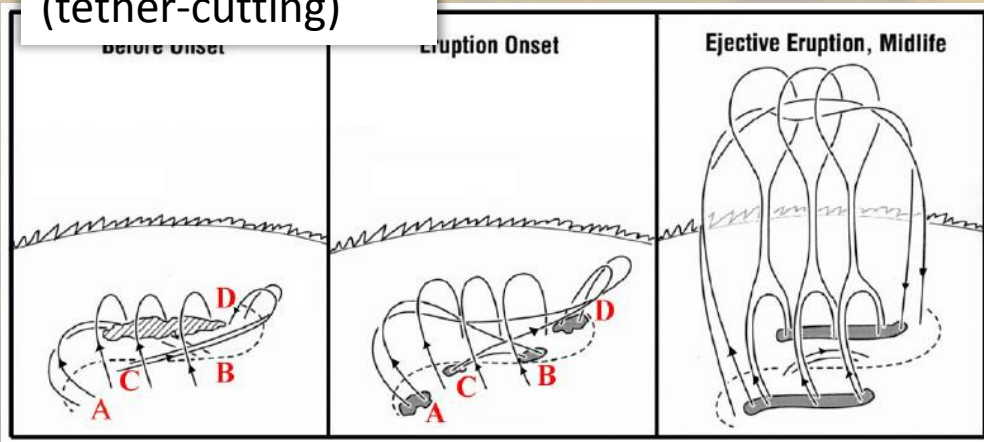
Sun, X., et al. 2015, ApJ 804, L28

Thalmann, J.K., et al. 2015, ApJ 801, L23

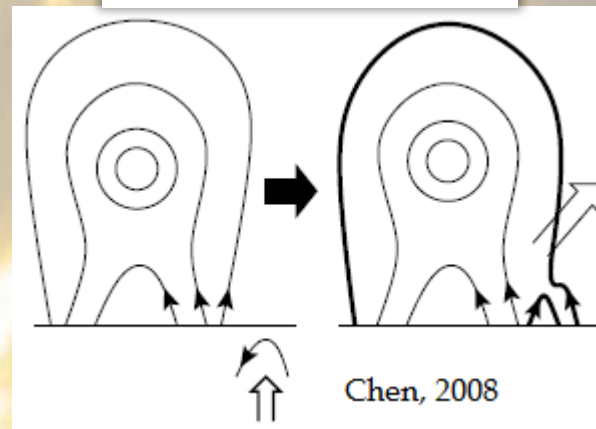


Triggering mechanisms

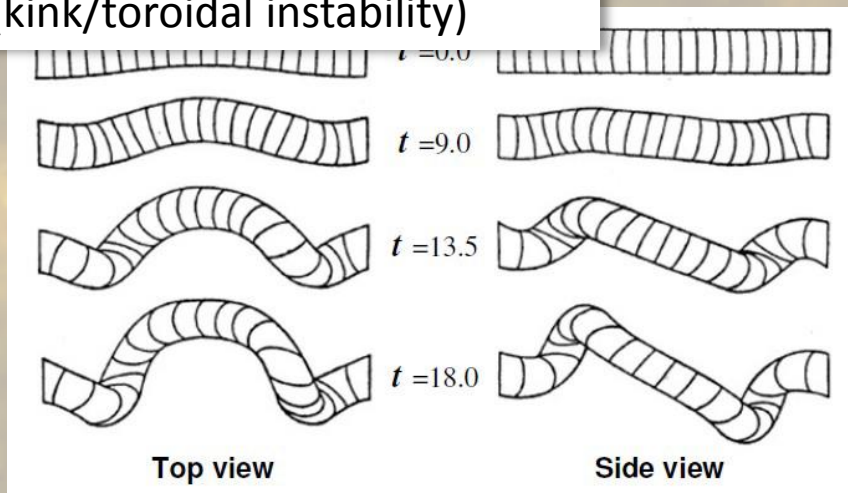
Przecięcie więzów (tether-cutting)



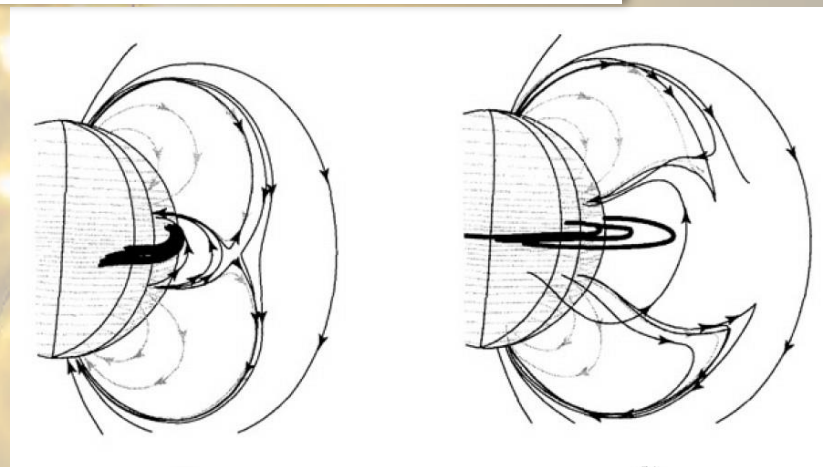
Wyptyw pola (flux emergence)



Niestabilność wyboczeniowa (kink/toroidal instability)

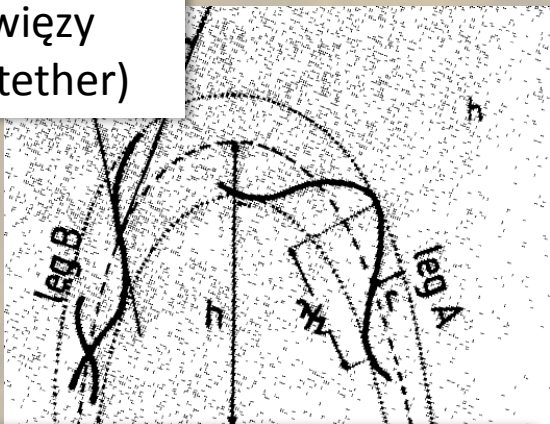


Przełamanie bariery (breakout)



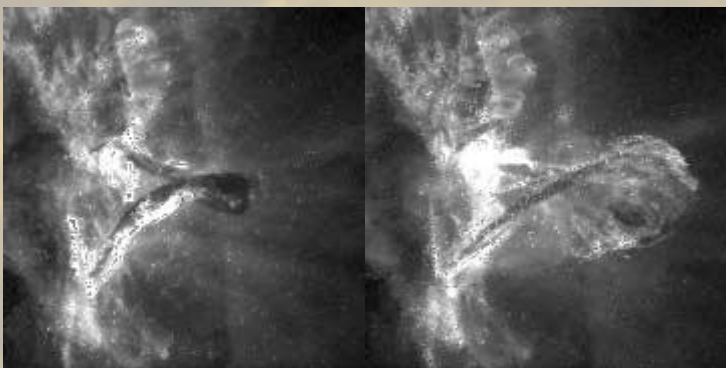
Braking mechanisms

Zbyt silne więzy
(confining tether)



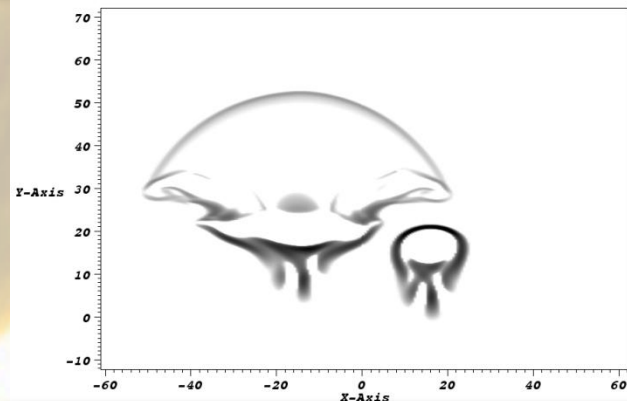
Vrsnak, B. 1990, Solar Phys. 129, 295

Niestabilność wyboczeniowa
(kink/toroidal instability)



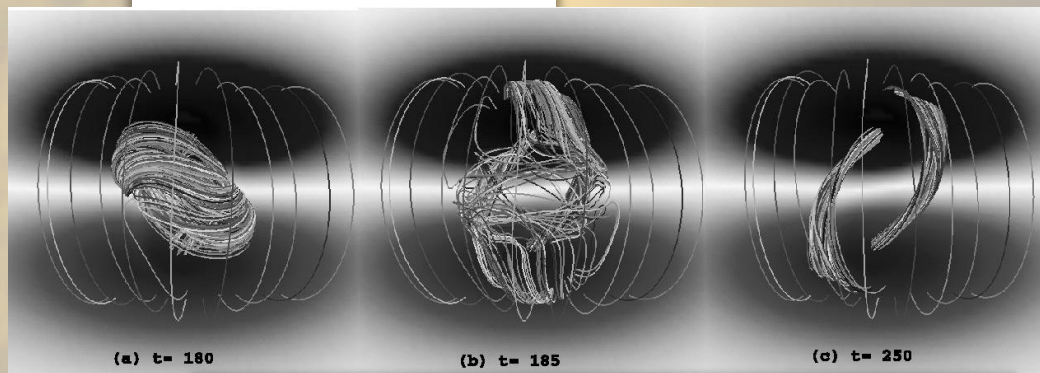
Ji, H. i in. 2003, ApJ, 595, L135

Wyptyw pola (flux emergence)



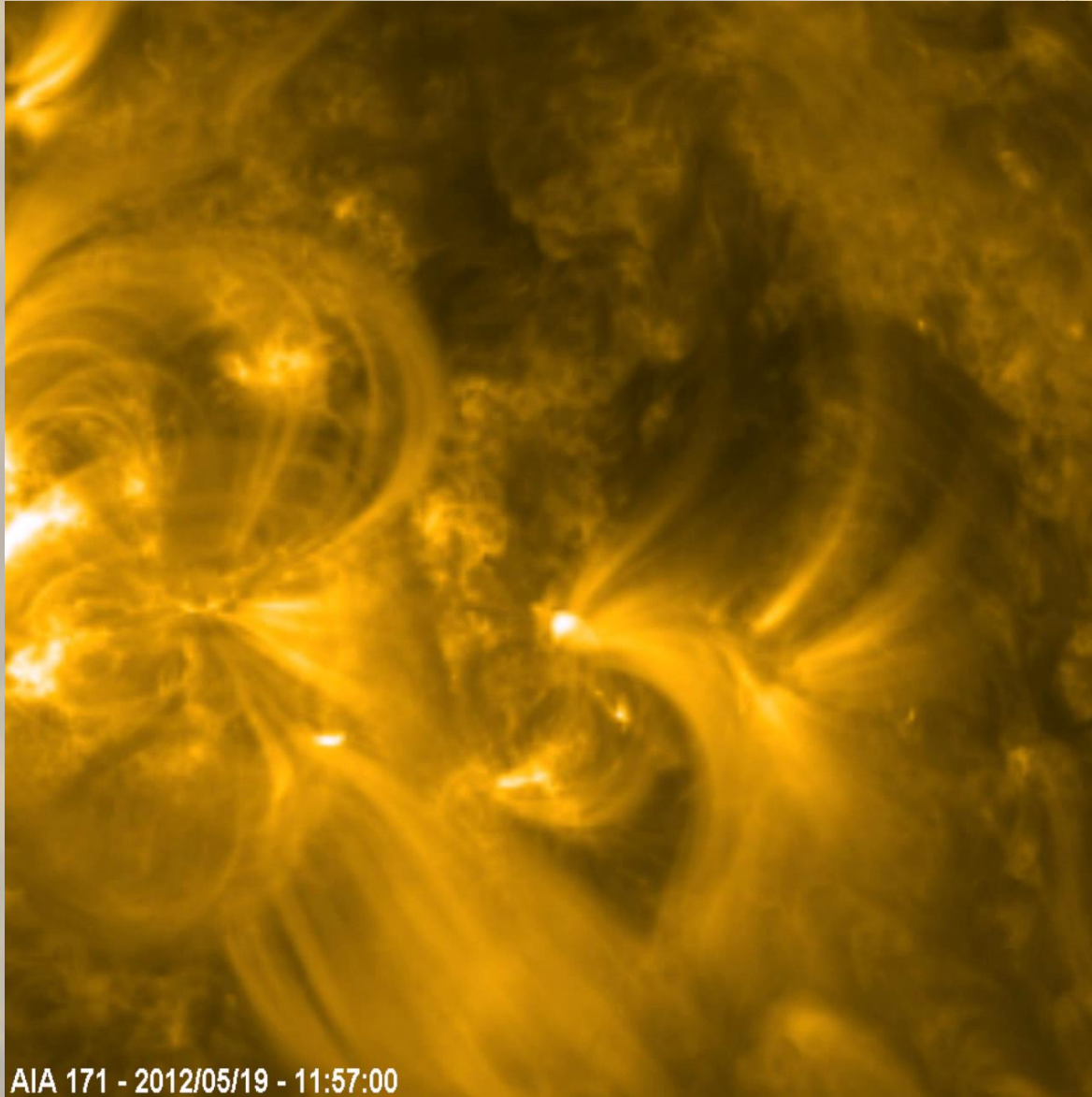
Archontis, V., et al. 2007, A&A 466, 367

Zderzenie z barierą
(barrier collision)



Amari, T., & Luciani, J.F. 1999, ApJ 515, L81

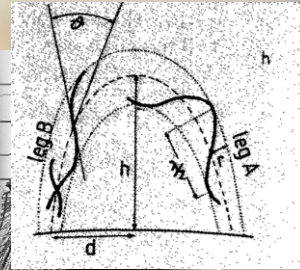
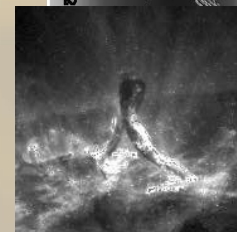
Which mechanism?



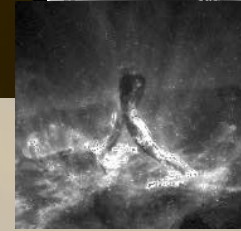
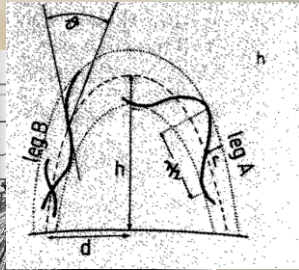
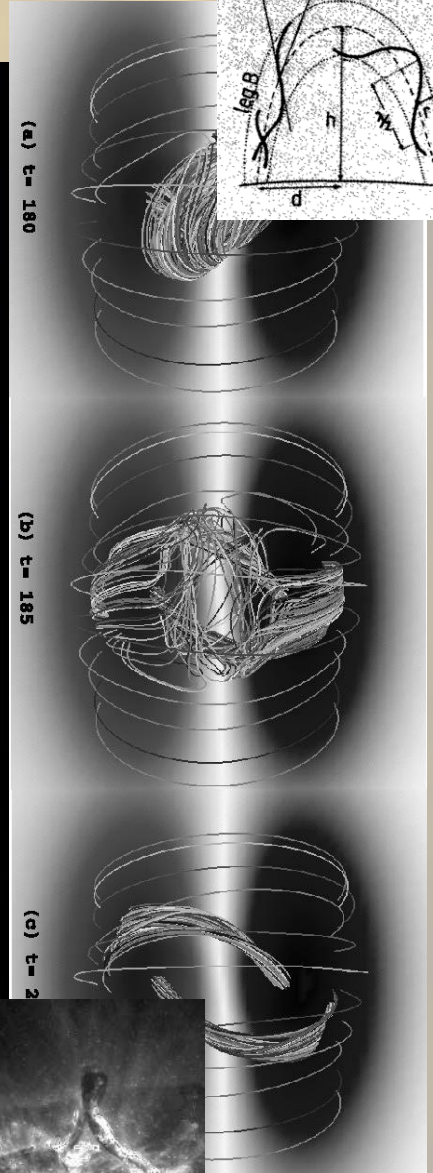
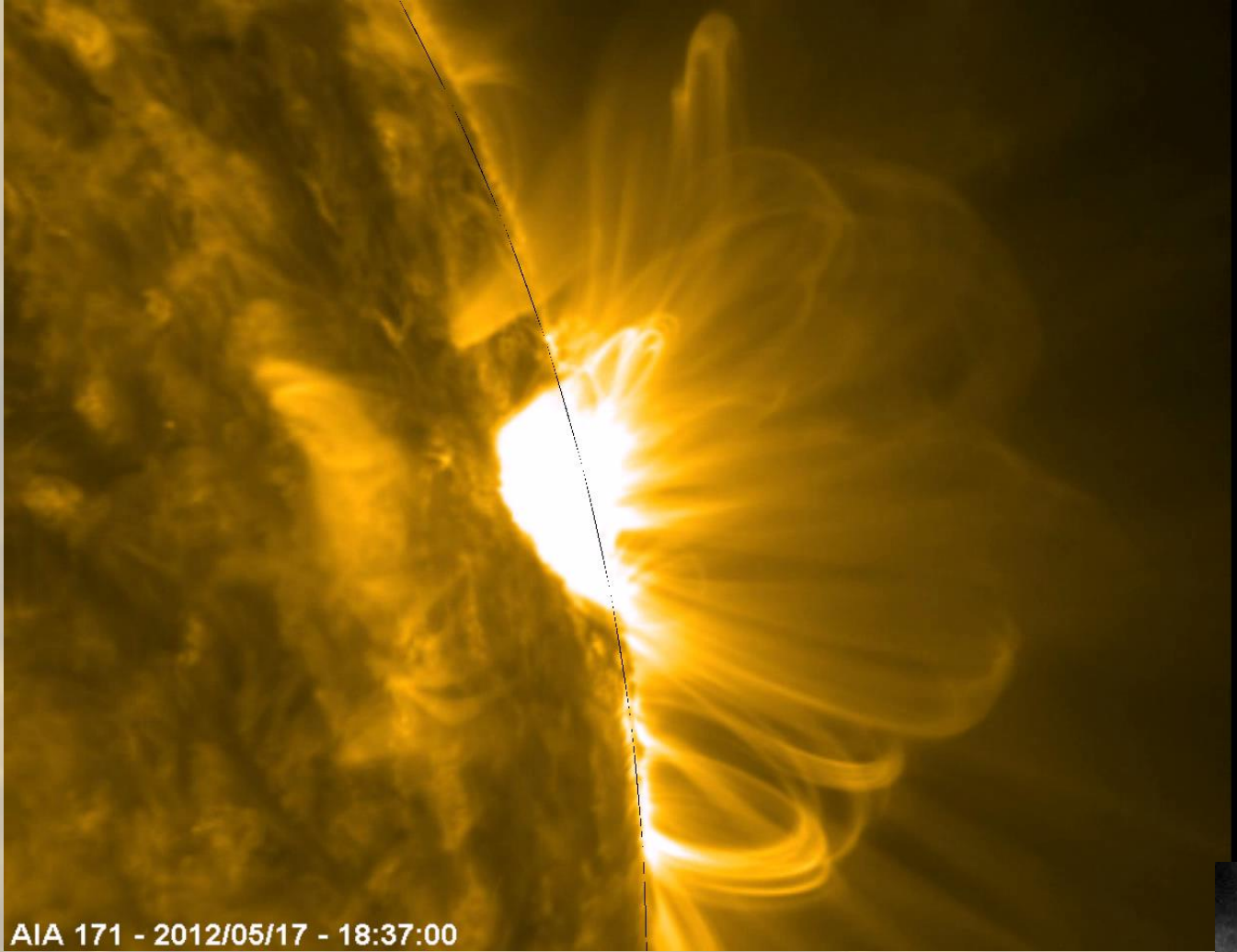
(a) $t = 180$

(b) $t = 185$

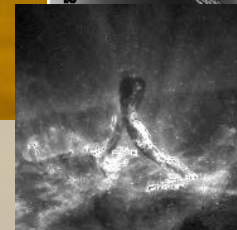
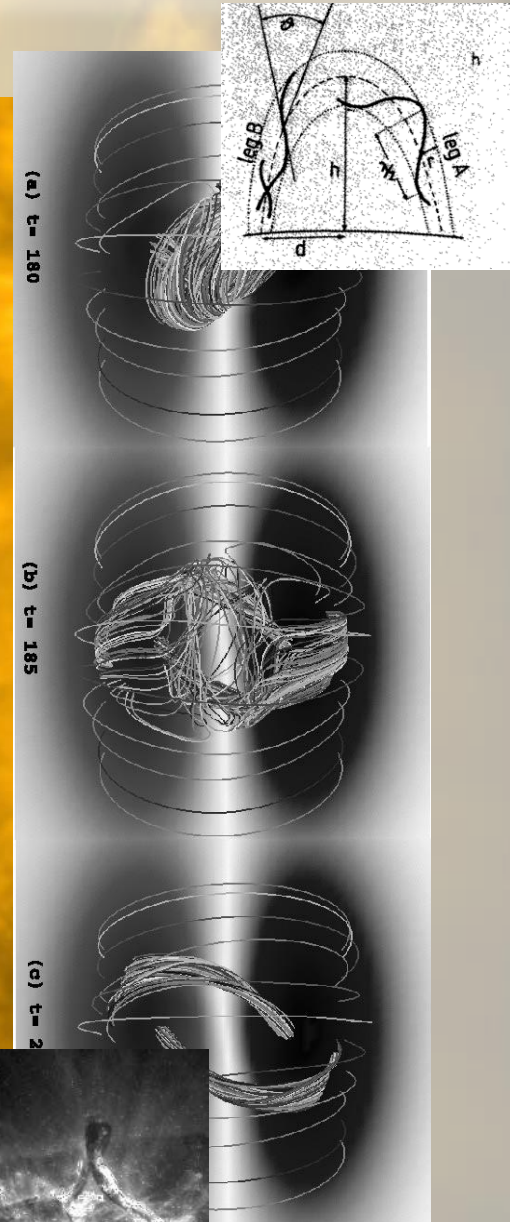
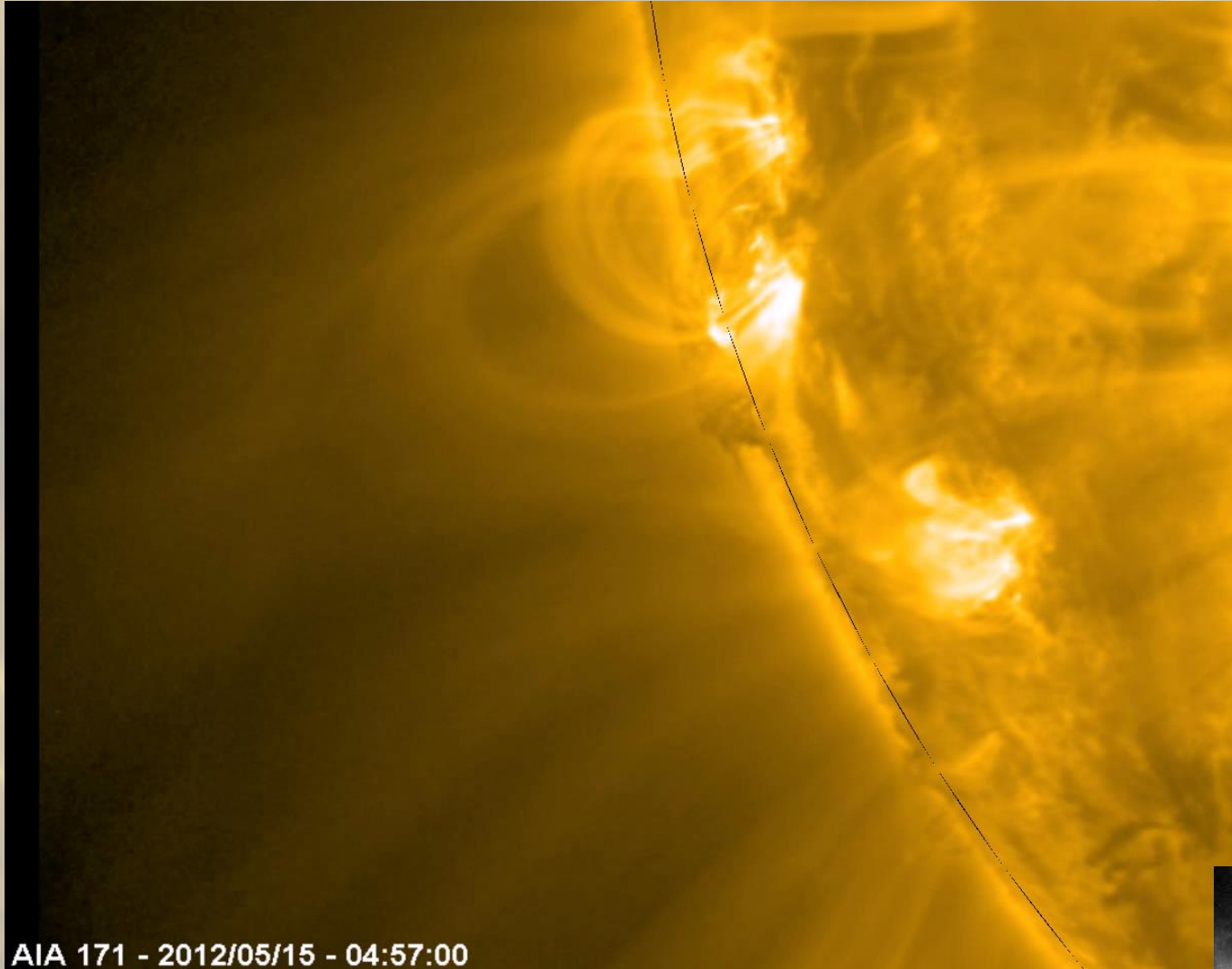
(c) $t = 200$



Which mechanism?

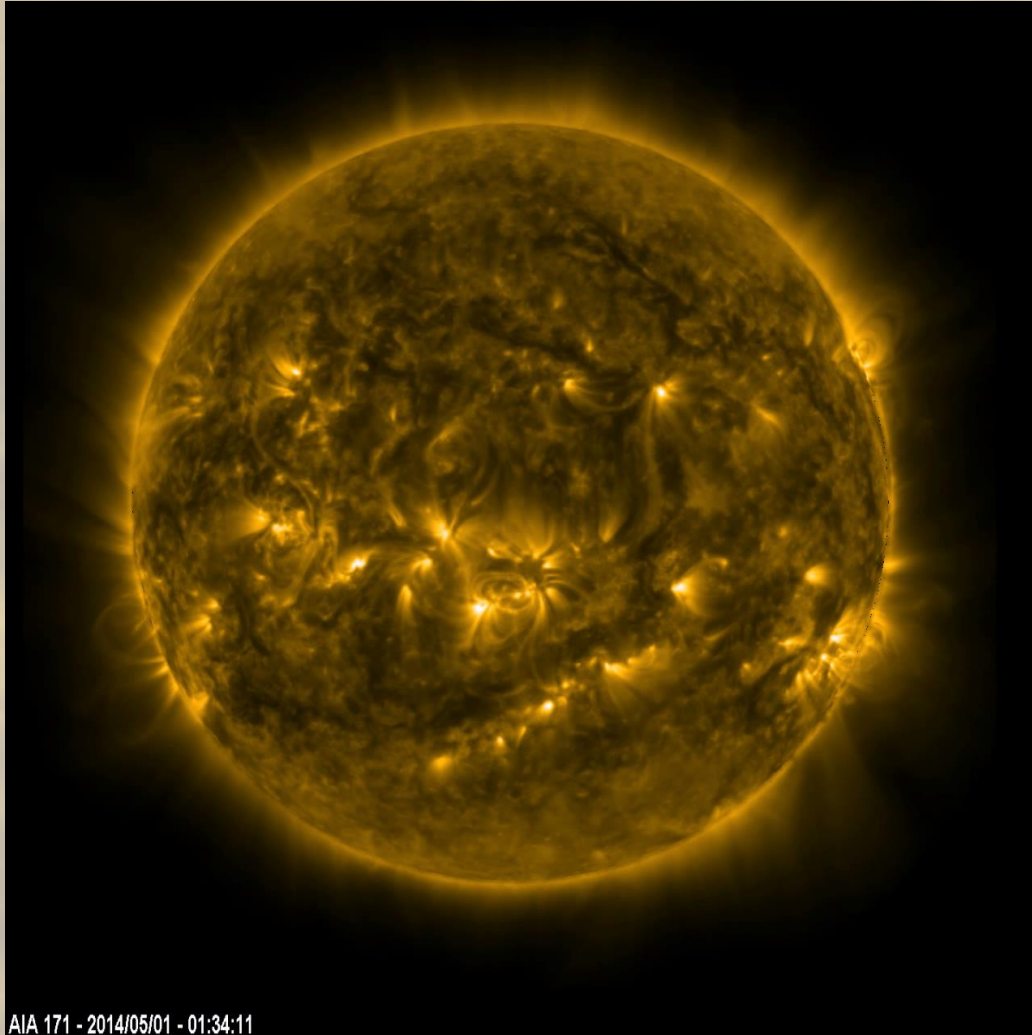


Which mechanism?



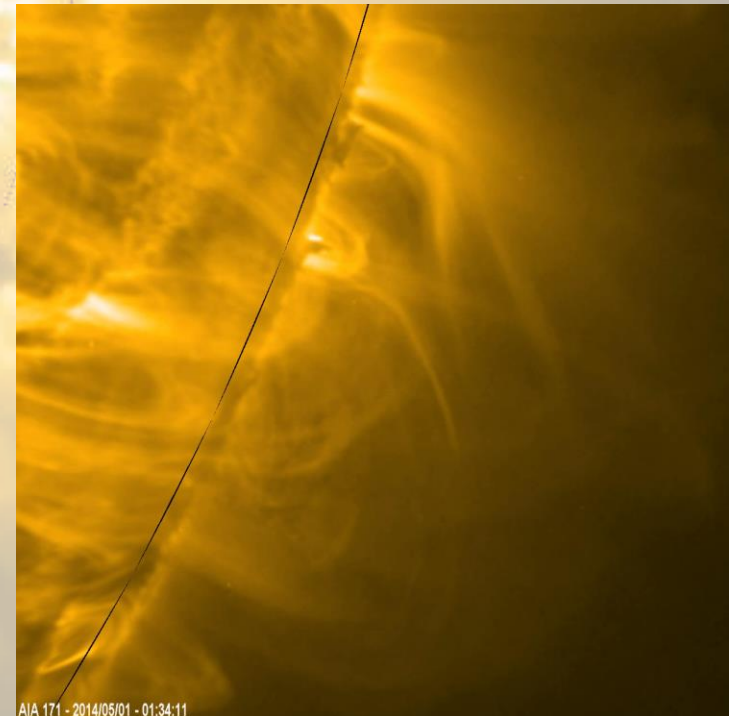
The aim

To construct method for automatic selection of eruptive/moving features on the basis of SDO/AIA observations.



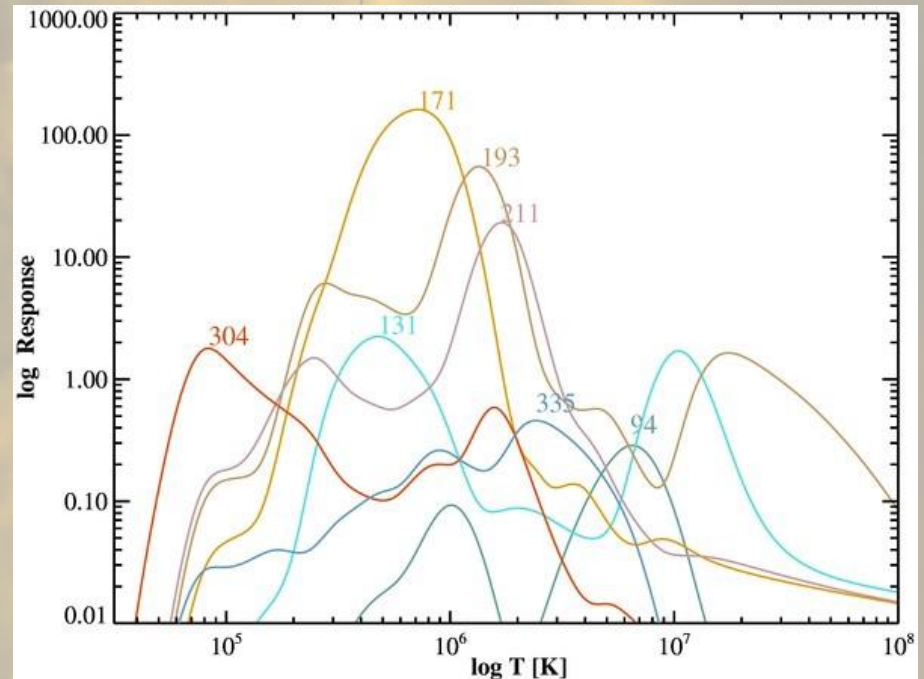
Human or machine?

- „by hand” searching – subjective
- crowdsourcing – extremely effective (galaxy zoo, Kepler lightcurves)
- machine do not discover new events
- new methods of machine learning



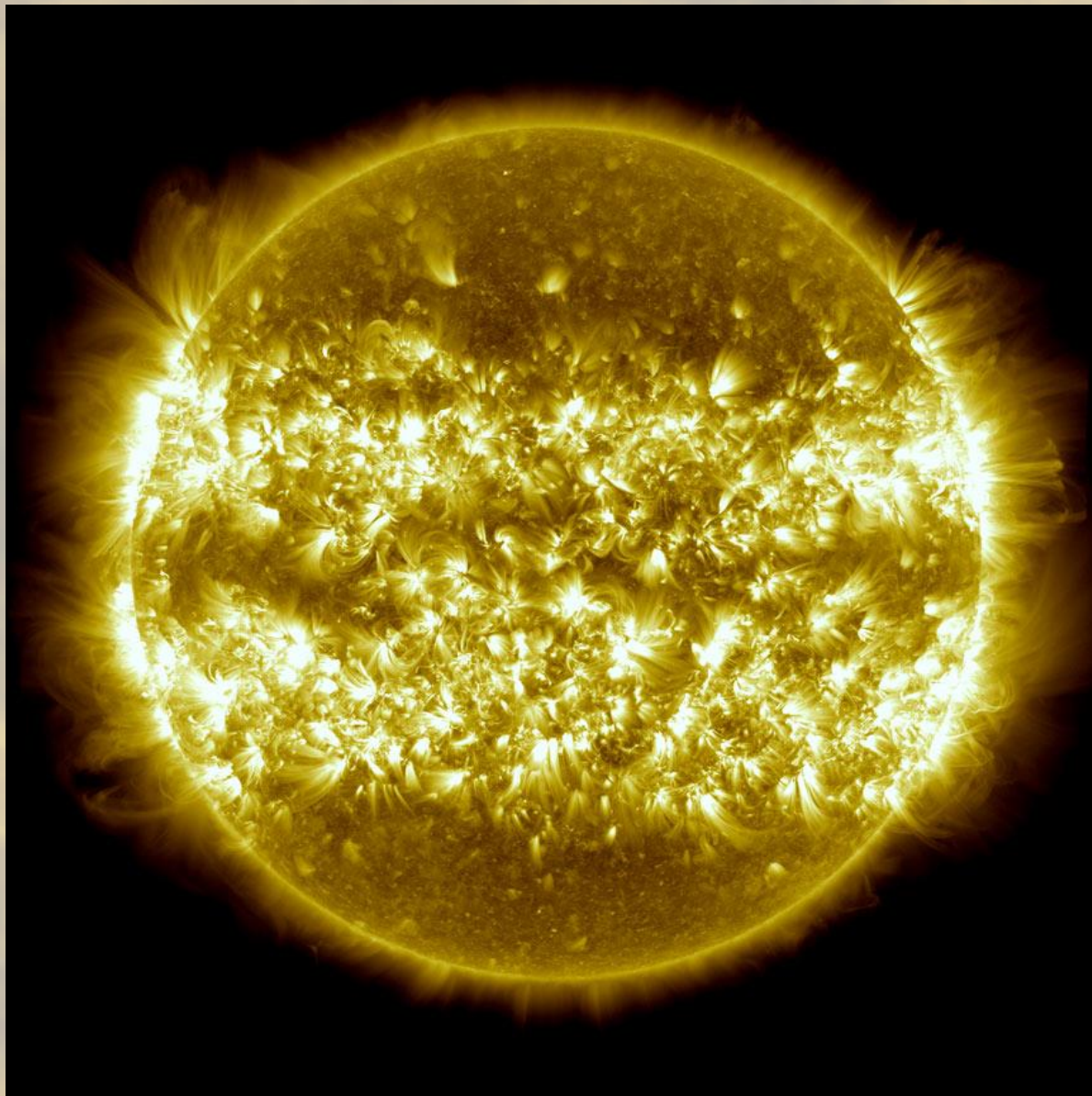
SDO/AIA

AIA wavelength channel	Source	Characteristic temperature
White light	continuum	5000 K
170 nm	continuum	5000 K
30.4 nm	He II	50,000 K
160 nm	C IV + continuum	10^5 & 5000 K
17.1 nm	Fe IX	6.3×10^5 K
19.3 nm	Fe XII, XXIV	1.2×10^6 & 2×10^7 K
21.1 nm	Fe XIV	2×10^6 K
33.5 nm	Fe XVI	2.5×10^6 K
9.4 nm	Fe XVIII	6.3×10^6 K
13.1 nm	Fe VIII, XX, XXIII	4×10^5 , 10^7 & 1.6×10^7 K



- 4 telescopes
- 4096 by 4096 full-disk images (0.6 arcsec/pixel)
- 12 s cadence
- 1.5 TB of data/day – basic problem for downloading and analysing data with automatic method

AIA - data products



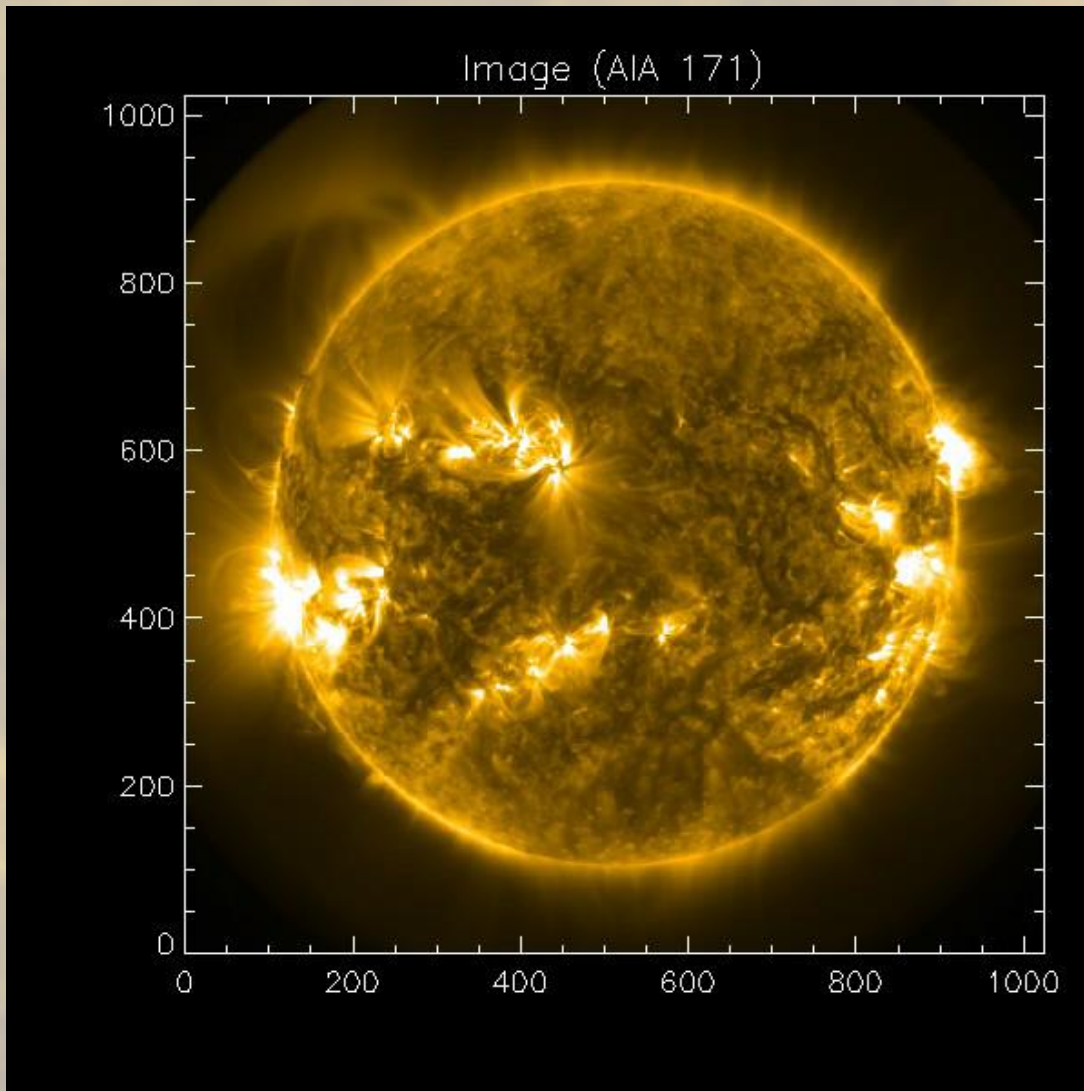
One uncompressed image
(Lev.1) – 32 MB

Lev.1.5 – after AIA_prep
(pointing correction, exp.
normalization)

Synoptic – Lev.1.5 compressed
to 1024x1024 pix., 2 min.
cadence – suitable for
searching of moving
structures, 1 MB/image

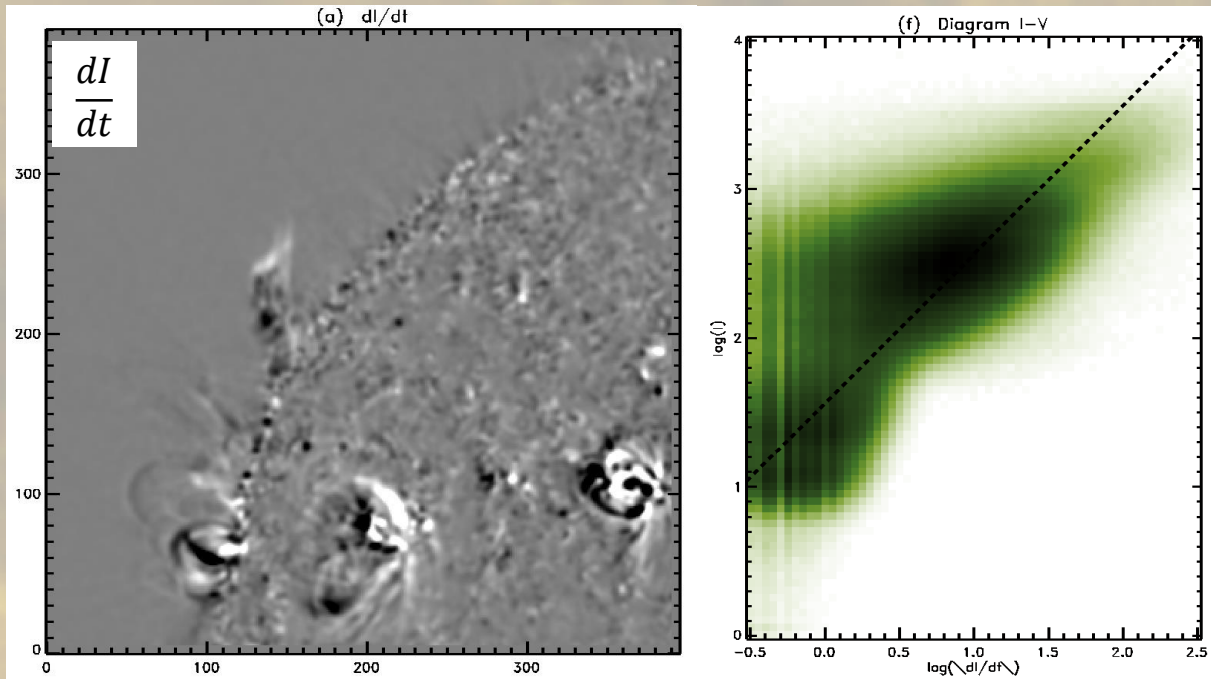
171 Å synoptic images have
been selected for eruption
searching

First step – data cube preparation



- 3 h-long series of synoptic data.
- Elimination of NaN pixels and empty images (dark frames) – removed pixels and frames were replaced with the ones obtained using the CONVOL function
- Last step is to blur images with gaussian filter (FWHM=2.8 pix)

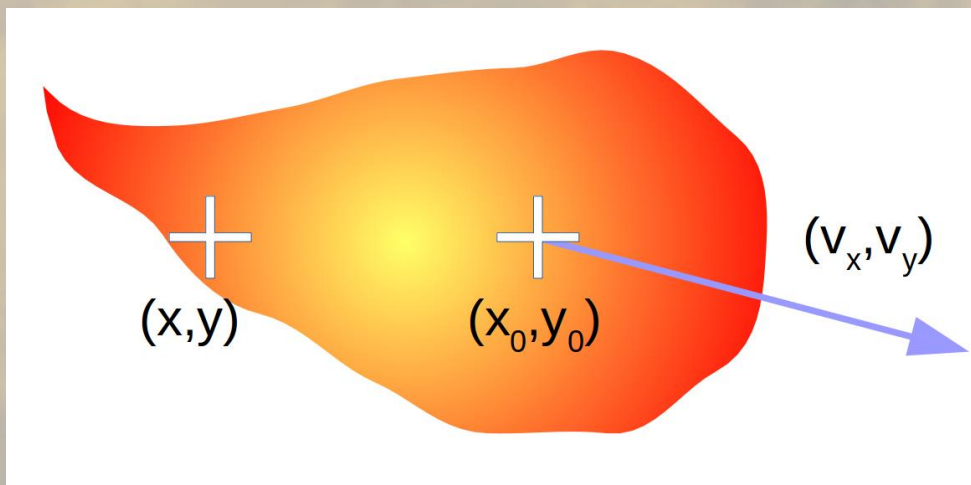
Standard approach – differential images



Most variable are brightest features.

It means that using derivative only will lead to detection of all bright features (loops, active regions) which is not our aim.

Moving structure



Moving feature with initial brightness distribution $R(x,y)$.

Its brightness is modulated with time by $\varphi(t)$.

Starting position (x_0, y_0) is moving with velocity (v_x, v_y) . Then brightness may be represented with:

$$I(x, y, t) = R(x - x_0, y - y_0)\varphi(t) = I_0(x, y)\varphi(t)$$

Differential image:

$$I_t = \frac{dI(x, y, t)}{dt} = -\varphi(t) \cdot (\vec{v} \circ \nabla I_0) + I_0 \frac{d\varphi(t)}{dt}$$

change of position

change of brightness

Moving structure

Let's look at two cases:

1. Stationary flare ($v = 0$).

Characteristic change rate is $\tau^{-1} = \frac{d}{dt} (\ln \varphi)$

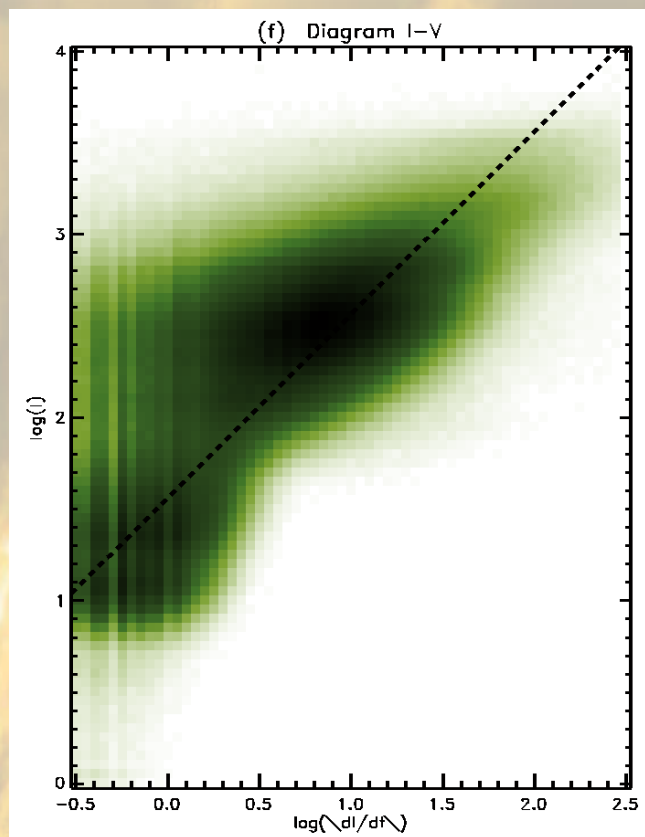
then:

$$I_t = I \frac{d \ln \varphi}{dt} = I \tau^{-1}$$

$$\log I_t = \log I - \log \tau$$

2. No changes of brightness ($I_0 \frac{d\phi(t)}{dt} = 0$).

We obtain: $I_t = -\vec{v} \cdot \nabla I$ which is a continuity equation ($\frac{d\rho}{dt} + \nabla \cdot \vec{j} = 0$) for uniform velocity field.



Moving structure

In practice for $I \rightarrow 0$ we get $I_t \neq 0$ due to noise. Therefore we add a constant value:

$$I_t^{norm} = \tau_\alpha^{-1} = \frac{I_t}{I + \alpha}$$

Operating on discrete values may produce uncertainties, therefore, for calculating derivative of normalized I, we use:

$$J(x, y, t) = \ln(I(x, y, t) + \alpha) - \ln \alpha$$

$$J_t = \frac{dJ}{dt} = \frac{d}{dt} (\ln(I + \alpha) - \ln \alpha) = \frac{dI}{dt} \frac{1}{I + \alpha} = \frac{I_t}{I + \alpha}$$

$$J_{tt} = \frac{d^2J}{dt^2} = \frac{d}{dt} \left(\frac{I_t}{I + \alpha} \right) = \frac{d^2I}{dt^2} \frac{1}{I + \alpha} - \left(\frac{I_t}{I + \alpha} \right)^2 = \frac{I_{tt}}{1 + \alpha} - J_t^2$$

Finally, we can calculate derivatives:

$$I_t^{norm} = \frac{I_t}{I + \alpha} = J_t$$

$$I_{tt}^{norm} = \frac{I_{tt}}{I + \alpha} = J_{tt} + J_t^2$$

Moving structure

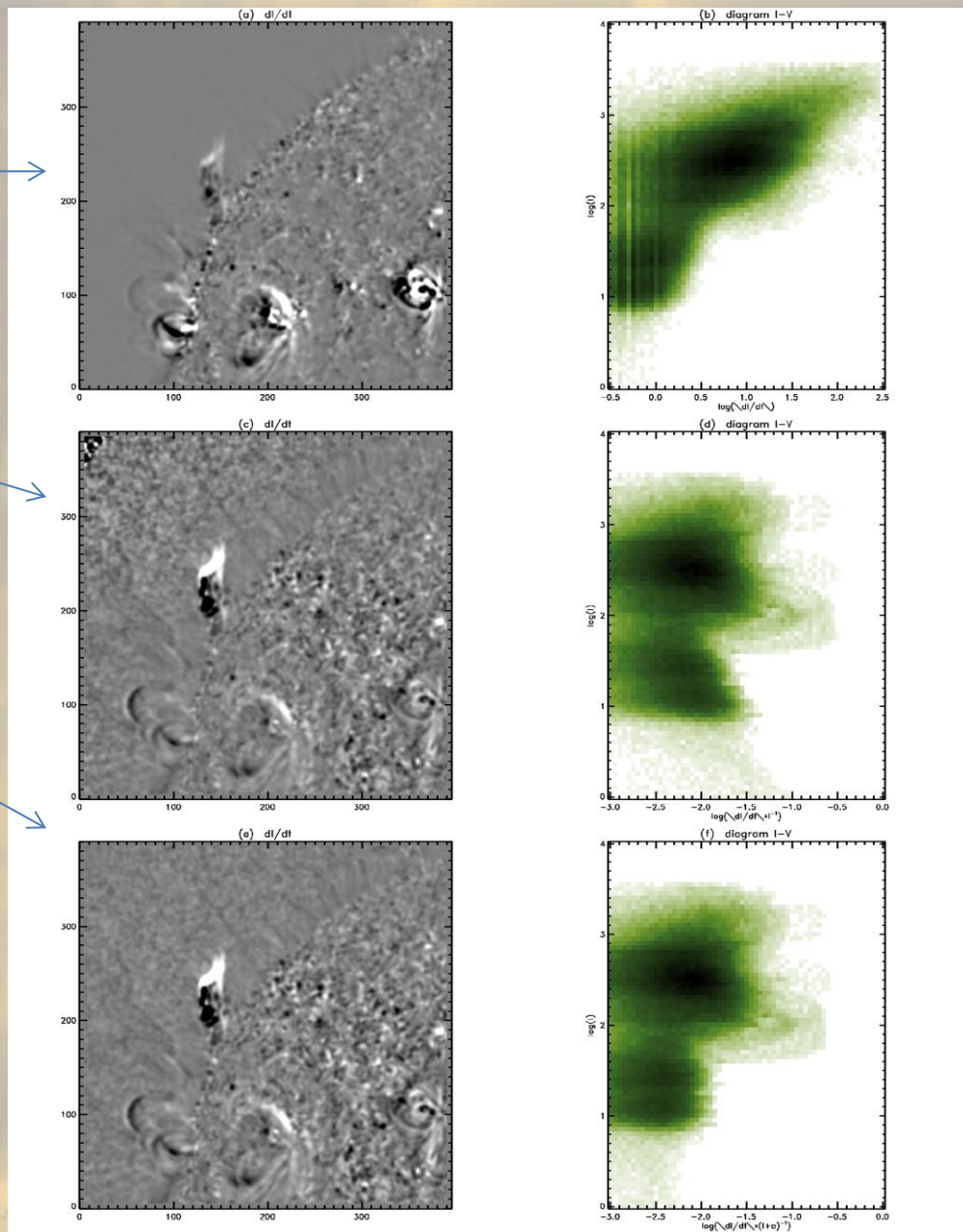
$$I_t$$

$$\frac{I_t}{I}$$

$$\frac{I_t}{I + \alpha}$$

For next step we constructed (arbitrarily) a variability index which was used to separate slow- and fast-changing structures:

$$V = \sqrt{J_t^2 + \frac{1}{4}J_{tt}^2}$$



Searching for eruptive events

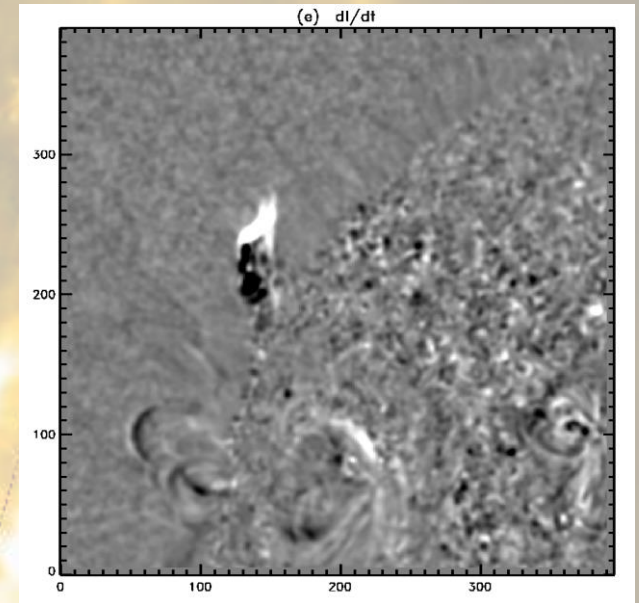
Defined value V may be used for eruptive events selection however it can't be done with one threshold value because it varies with solar cycle, location on the disk etc.

For this purpose we used Bayes theorem:

$$P(C_n|x) = \frac{P(x, C_n)}{P(x)} = \frac{P(x|C_n)P(C_n)}{\sum_{i=0}^N P(x|C_i)P(C_i)}$$

We have measured value x , which we want to classify as one of C_i . We know probability of measuring x belonging to class C_i ($P(x|C_i)$) and global probability of occurrence of each class.

In our problem of image analysis we defined two classes: E (eruptive), and Q (quiet). On the basis of measured state of each pixel $\hat{x} = (I, V)$ we want to classify it to one of classes E or Q.



Searching for eruptive events

In theory we know $P(\hat{x}, E)$ and $P(\hat{x}, Q)$, so measuring \hat{x} we can calculate $P(E|\hat{x})$ and $P(Q|\hat{x})$ immediately, and assign class.

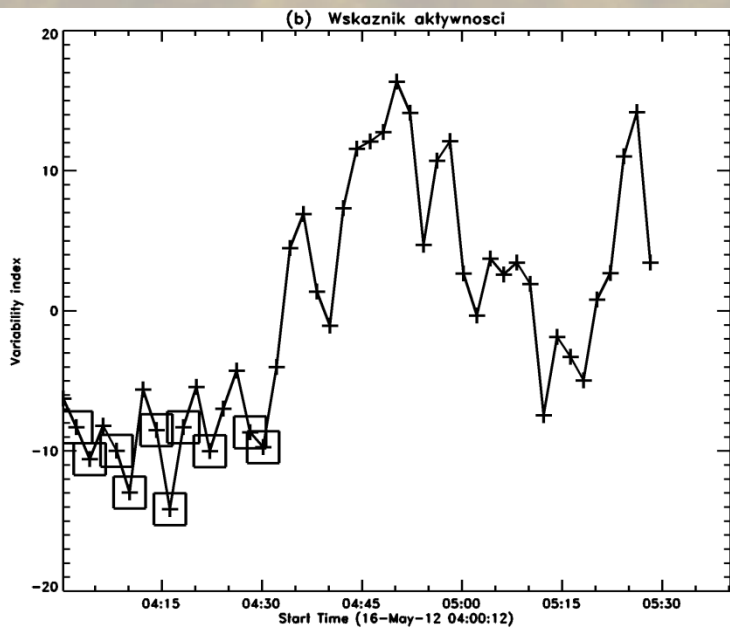
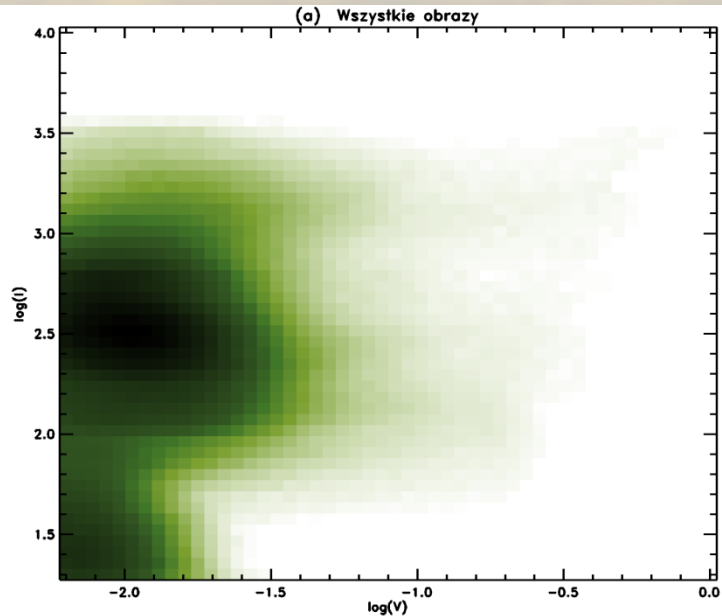
However, in practice, we do not know probability $P(\hat{x}, E)$, but we can estimate $P(\hat{x}|Q)$ assuming that several images in sequence do not contain eruptions.

For this purpose we used mean values of pixel brightness ($I_{mean}(t)$) and variability index ($V_{mean}(t)$):

$$I_{mean}(t_k) = \frac{1}{n_x n_y} \sum_{i=1}^{n_x} \sum_{j=1}^{n_y} I(x_i, y_j, t_k)$$

$$V_{mean}(t_k) = \frac{1}{n_x n_y} \sum_{i=1}^{n_x} \sum_{j=1}^{n_y} V(x_i, y_j, t_k)$$

Searching for eruptive events



We defined activity index ($A(t_i)$) as a weighted sum ($w=8$):

$$A(t_i) = \frac{I_{mean}(t_k) - \overline{I_{mean}}}{\sigma_{I_{mean}}} + w \frac{V_{mean}(t_k) - \overline{V_{mean}}}{\sigma_{V_{mean}}}$$

20% of frames with lowest values of $A(t_i)$ were used for estimation of $P(\hat{x}|Q)$. We can calculate:

$$P(\hat{x}, E) \approx P(\hat{x}) - P(\hat{x}, Q) = P(\hat{x}) - P(\hat{x}|Q)P(Q)$$

where $P(\hat{x})$ is normalized distribution of $\hat{x} = (I, V)$ for entire sequence of images.

$P(Q)$, which is probability that randomly selected pixel belong to class „no eruption”, was calculated iteratively as follows.

Searching for eruptive events

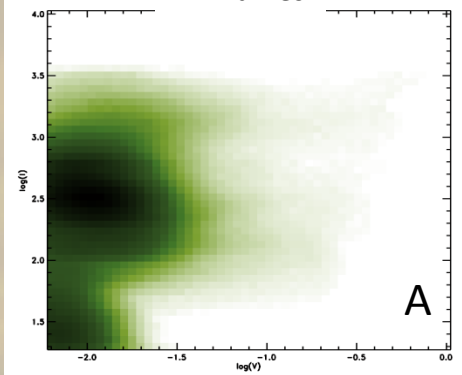
Let's assume that $P(Q) \approx 1$, and classify pixels as Q or E. Having number of E-pixels we calculate $P(Q) = 1 - P(E) = 1 - \frac{n_{erupt}}{n_{total}}$, and run algorithm again with new value of $P(Q)$. Usually, after 3 steps $P(Q)$ had stabilized.

Finally, we can calculate probability that pixel of state $\hat{x} = (I, V)$ belongs to class E:

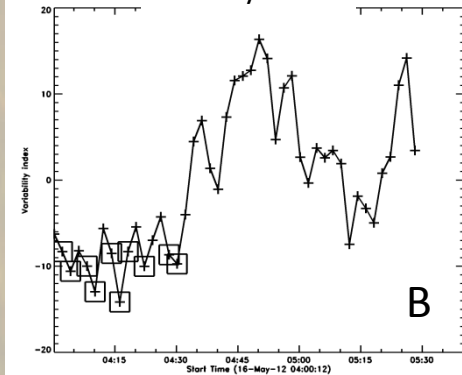
$$P(E|\hat{x}) = \frac{P(\hat{x}, E)}{P(\hat{x})} = \frac{P(\hat{x}) - P(\hat{x}, Q)}{P(\hat{x})} = 1 - \frac{P(Q)P(\hat{x}|Q)}{P(\hat{x})}$$

Algorithm

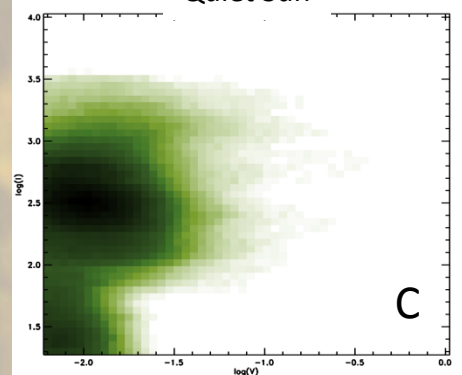
All frames



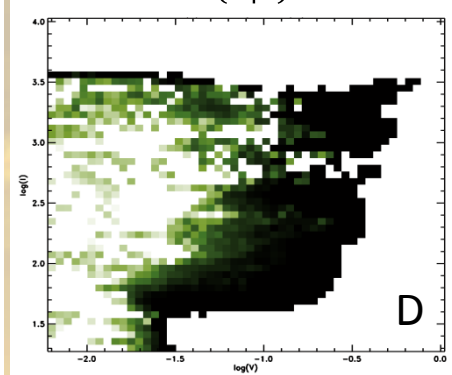
Activity index



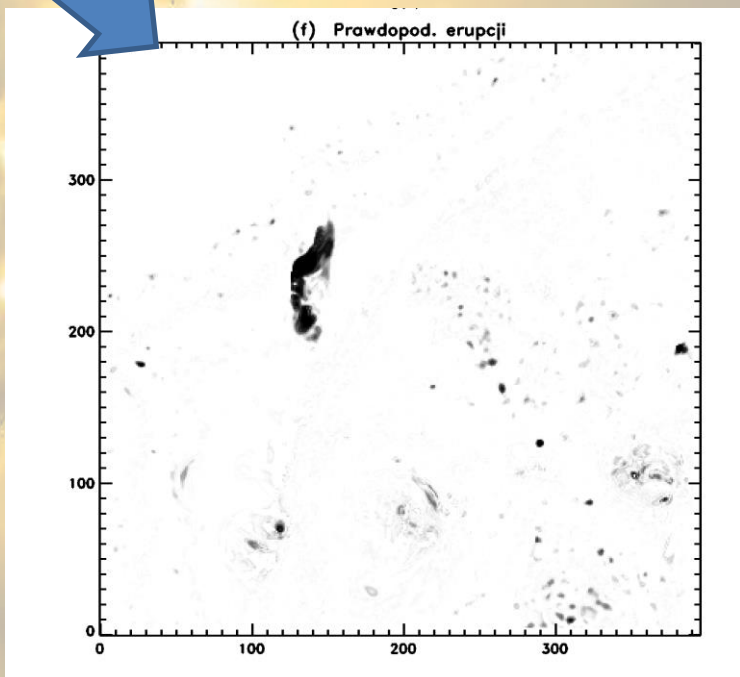
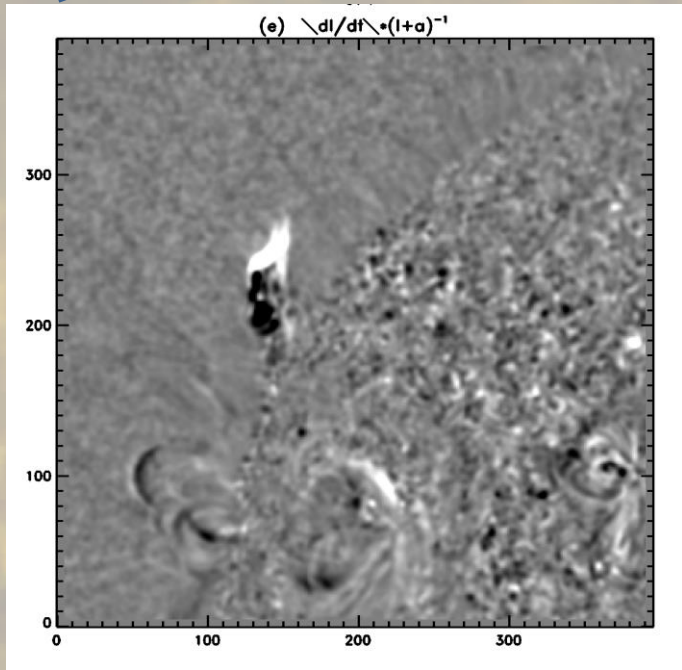
Quiet Sun



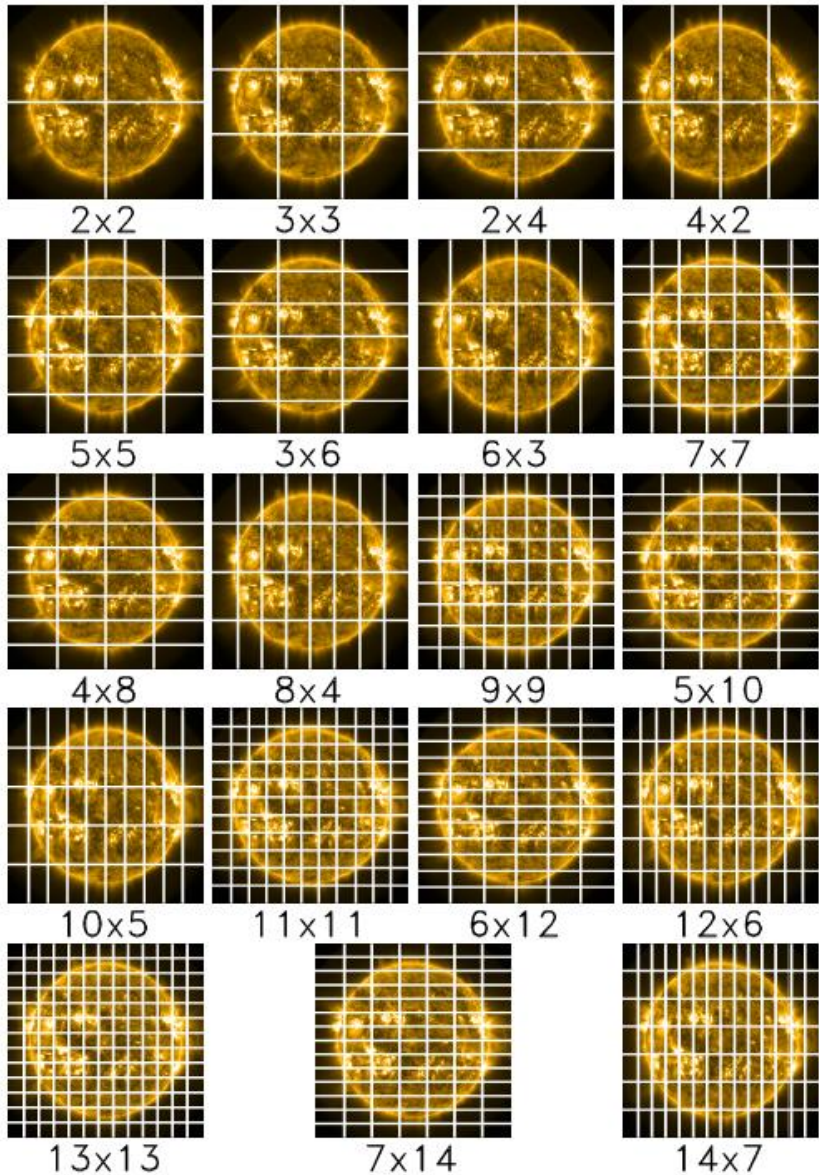
$P(E|\hat{x})$



$$A \frac{B}{C} = D$$



Algorithm



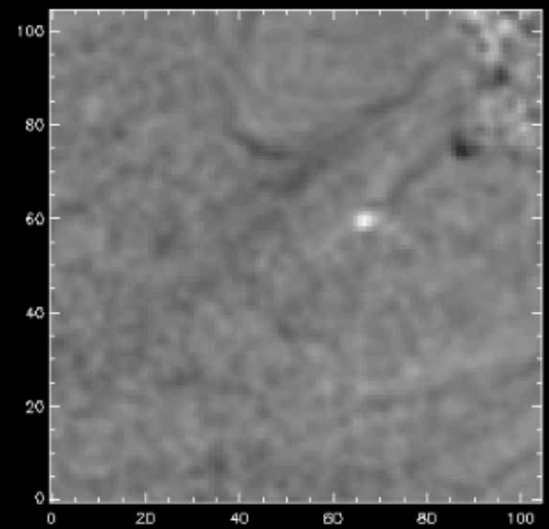
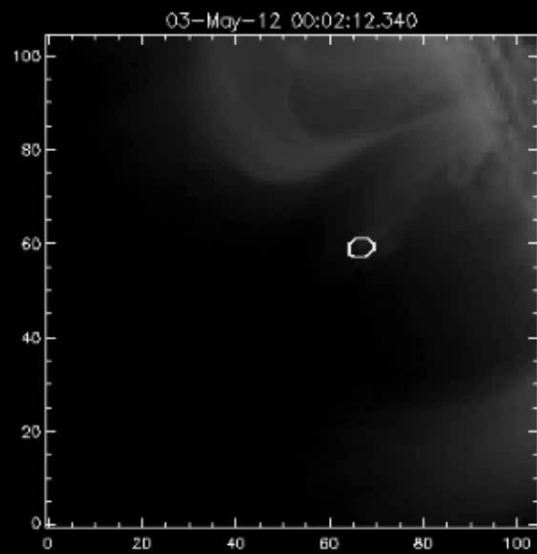
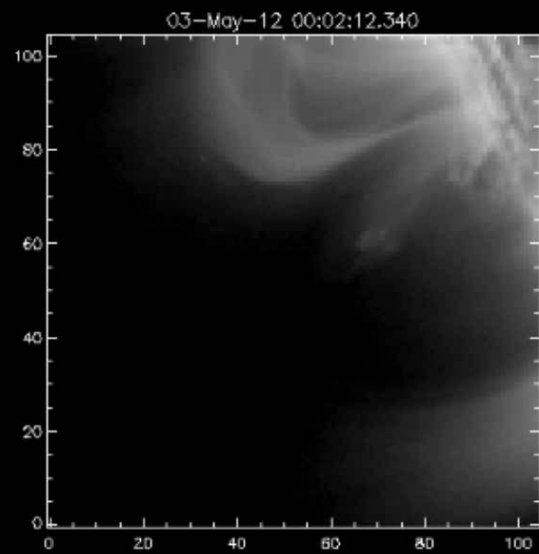
E-pixels were searched within frames of various size to avoid edge effects.

Area of eruption was calculated with simplest growth algorithm.

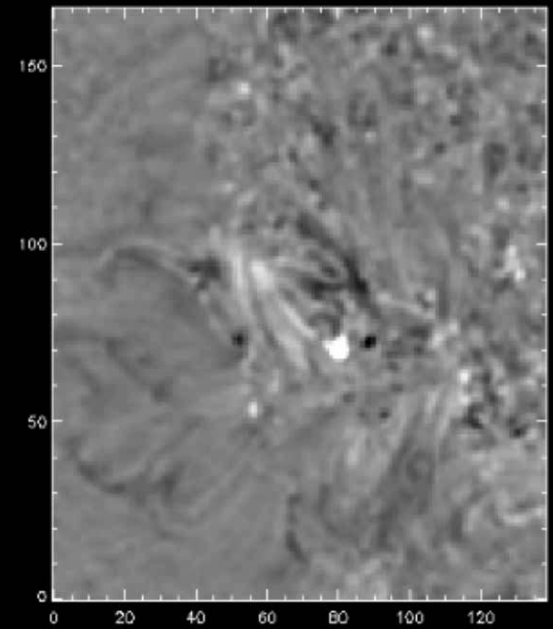
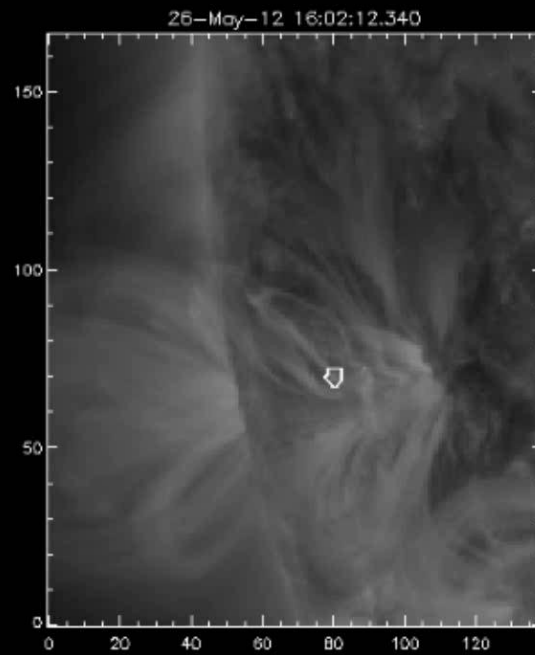
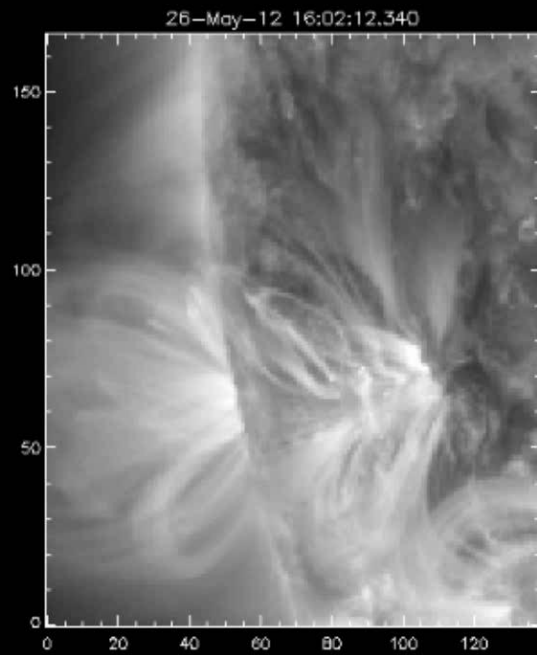
Possible eruption was recognized when selected area:

1. for each pixel: $P(E|\hat{x}) > 0.35$
2. was visible on 8 or more frames consecutive frames
3. was greater than 600 arcsec^2 on at least one frame
4. mean value of brightness was above 30 DN on at least one frame
5. showed change of centroid position greater than 25 arcsec.

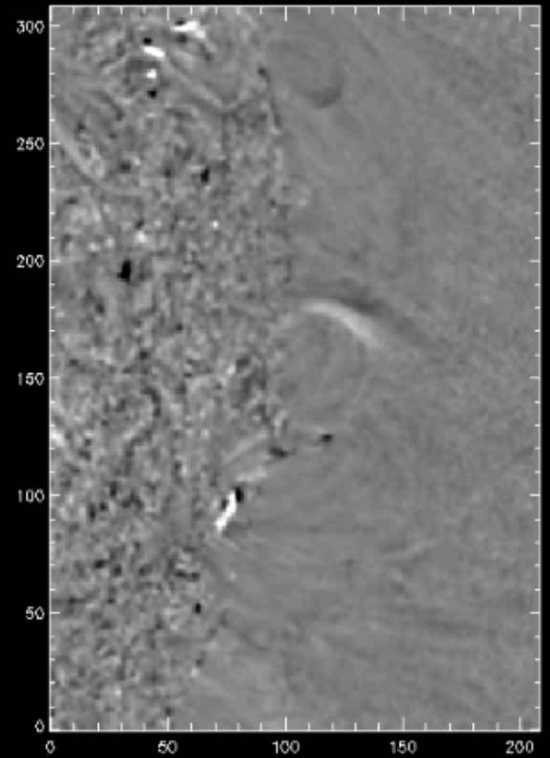
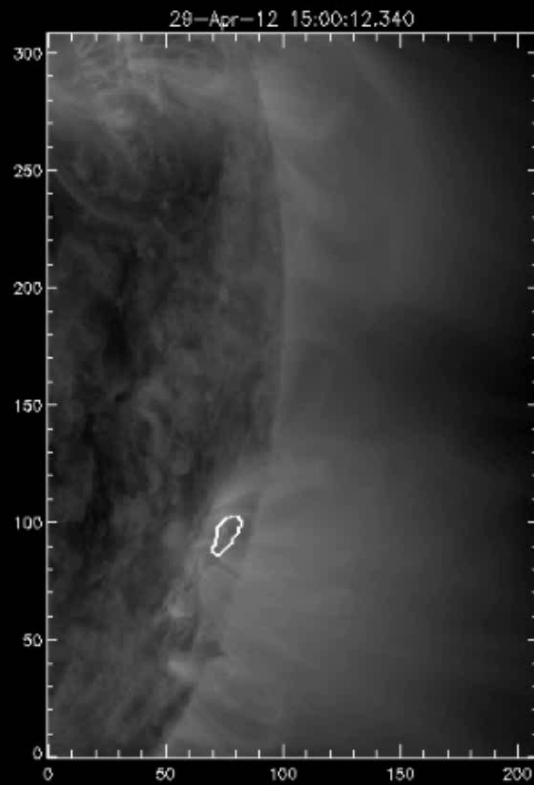
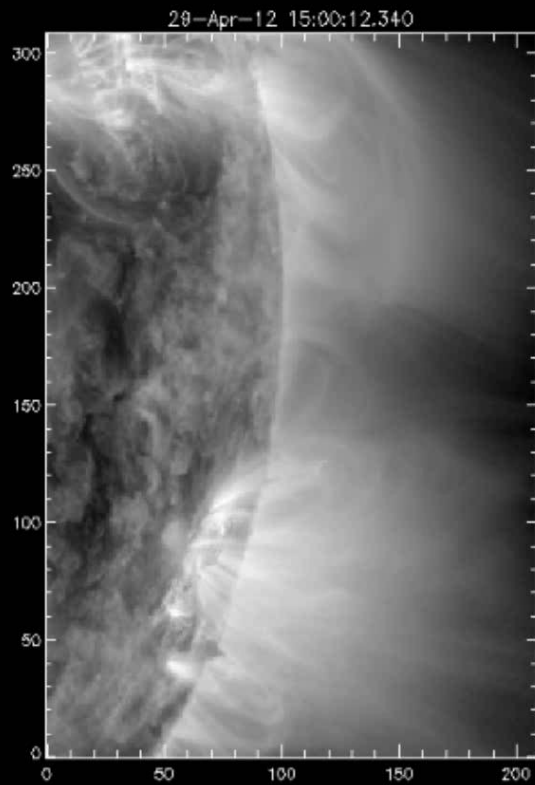
Example



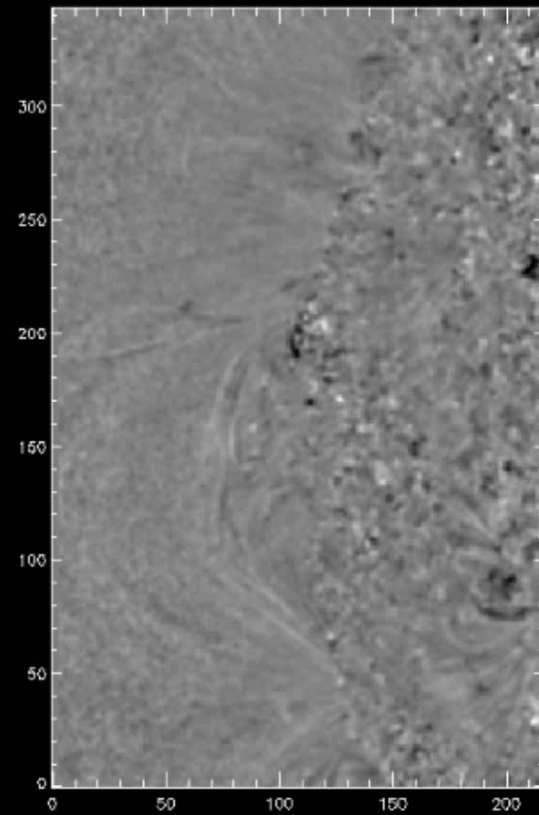
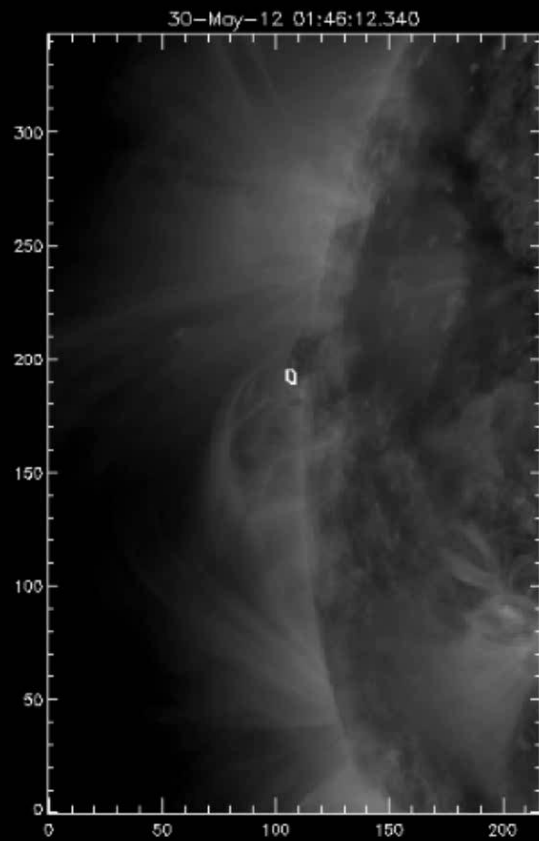
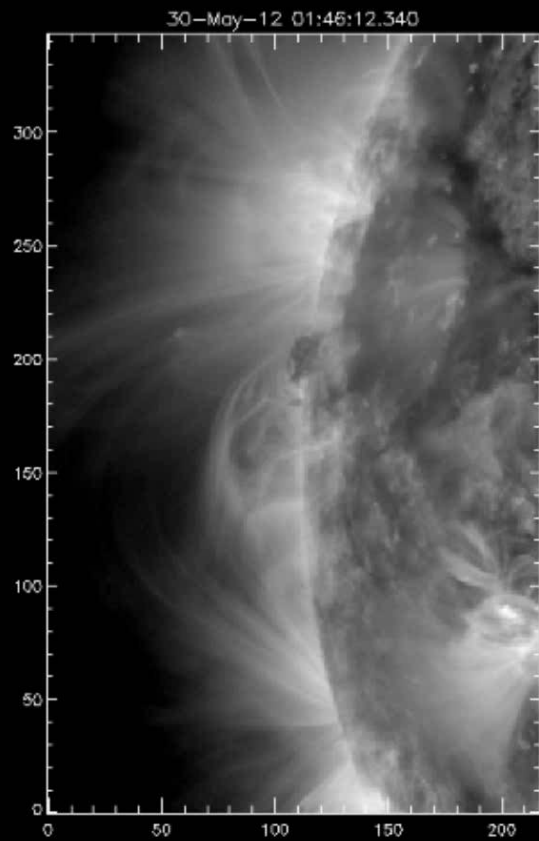
Example



Example



Output



Output

Pole	Typ danych	Jednostka	Opis
ID	LONG	-	(nie używany)
T_START	DOUBLE	sekundy	Czas początku zjawiska (w formacie anytim)
T_END	DOUBLE	sekundy	Czas końca zjawiska (w formacie anytim)
T_PEAK	DOUBLE	sekundy	Czas osiągnięcia największej powierzchni (w formacie anytim)
DURATION	FLOAT	sekundy	Czas trwania zjawiska
WAVE	LONG	Å	Długość fali filtra SDO/AIA w którym zarejestrowano zjawisko
N_POINTS	LONG	-	Liczba obrazów, na których zarejestrowano zjawisko
MASK	BYTE[80]	-	Tablica, w której pierwsze N_POINTS elementów ma wartość 1, zaś pozostałe 0
MASK_SEQ	BYTE[80]	-	(nie używany)
TIMES	DOUBLE[80]	sekundy	Czasy rejestracji poszczególnych obrazów (w formacie anytim)
X_CENTER	FLOAT[80]	arcsec	Położenie geometrycznego środka masy obszaru erupcji w osi X
X_CENTER_M	FLOAT	arcsec	Uśrednione położenie środka masy obszaru erupcji w osi X
X_START	FLOAT	arcsec	Współrzędna X miejsca startu erupcji
Y_CENTER	FLOAT[80]	arcsec	Położenie środka masy obszaru erupcji w osi Y
Y_CENTER_M	FLOAT	arcsec	Uśrednione położenie środka masy obszaru erupcji w osi Y
Y_START	FLOAT	arcsec	Współrzędna Y miejsca startu erupcji
IS_ERUPTION	INT	logiczna	Czy zjawisko jest erupcją? (nie używany – zawsze <i>true</i>)
H_FRONT	FLOAT[80]	arcsec	Odległość frontu erupcji od miejsca startu mierzona wzdłuż prostej wyznaczającej średni kierunek ruchu erupcji
H_CENTER	FLOAT[80]	arcsec	Odległość geometrycznego środka masy obszaru erupcji od miejsca startu mierzona wzdłuż prostej wyznaczającej średni kierunek ruchu erupcji

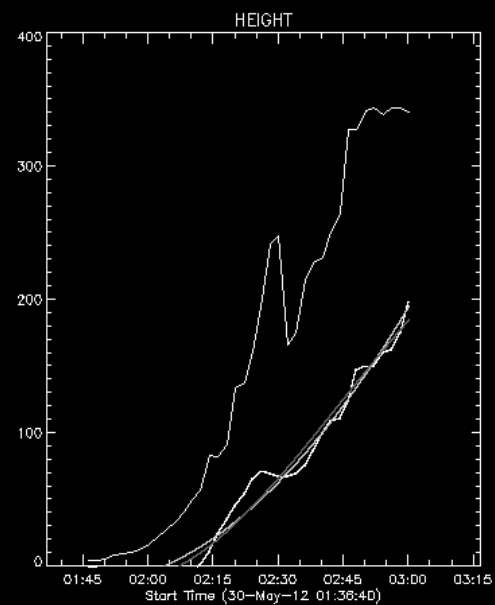
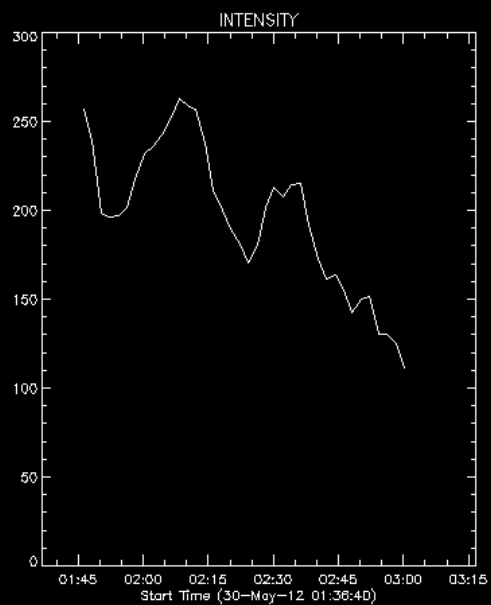
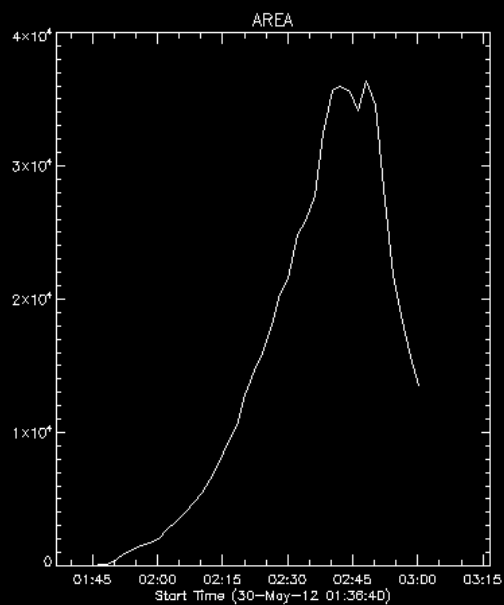
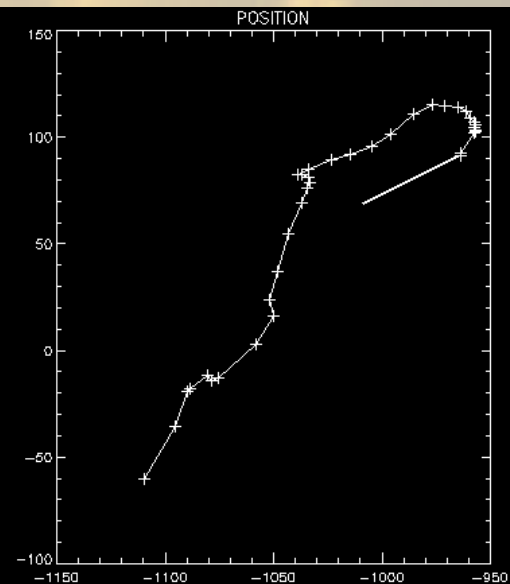
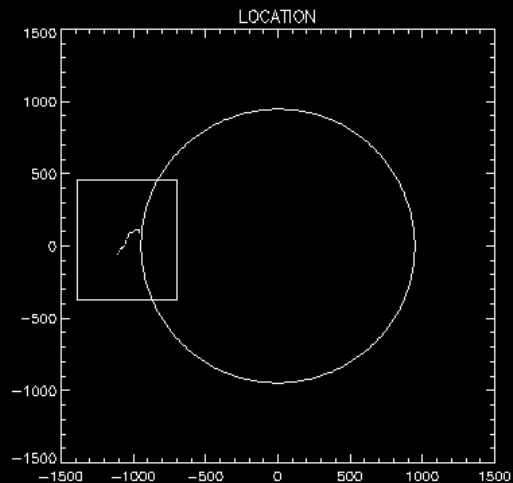
Pole	Typ danych	Jednostka	Opis
H_BOTTOM	FLOAT[80]	arcsec	Odległość spodu erupcji od miejsca startu mierzona wzdłuż prostej wyznaczającej średni kierunek ruchu erupcji
H_TRAJECT_2	FLOAT[3]	-	Współczynniki wielomianu drugiego stopnia dopasowanego do trajektorii geometrycznego środka masy (H_CENTER)
H_TRAJECT_3	FLOAT[4]	-	Współczynniki wielomianu trzeciego stopnia dopasowanego do trajektorii geometrycznego środka masy (H_CENTER)
X_VERSOR	FLOAT	-	Składowa X wersora wyznaczającego średni kierunek ruchu erupcji
Y_VERSOR	FLOAT	-	Składowa Y wersora wyznaczającego średni kierunek ruchu erupcji
AREA	FLOAT[80]	arcsec ²	Powierzchnia kątowna zajmowana przez erupcję
AREA_M	FLOAT	arcsec ²	Średnia powierzchnia kątowna erupcji
AREA_X	FLOAT	arcsec ²	Maksymalna powierzchnia kątowna osiągnięta przez erupcję
INTENS	FLOAT[80]	DN	Średnie natężenie sygnału w obszarze erupcji
INTENS_M	FLOAT	DN	Średnie natężenie sygnału podczas trwania erupcji
INTENS_X	FLOAT	DN	Maksymalne natężenie sygnału osiągnięte w obszarze erupcji
DIFF_T	FLOAT[80]	DN	Średnia wartość obrazu różnicowego w obszarze erupcji
N_DIFF_T	FLOAT[80]	-	Średnia wartość znormalizowanego obrazu różnicowego w obszarze erupcji – patrz wzór (3.11)
F_VAR	FLOAT[80]	-	Średnia wartość wskaźnika zmienności w obszarze erupcji – patrz wzór (3.15)
F_VAR_M	FLOAT	-	Średnia wartość wskaźnika zmienności w czasie trwania erupcji
NOTHING	INT	-	(nie używany)

Output

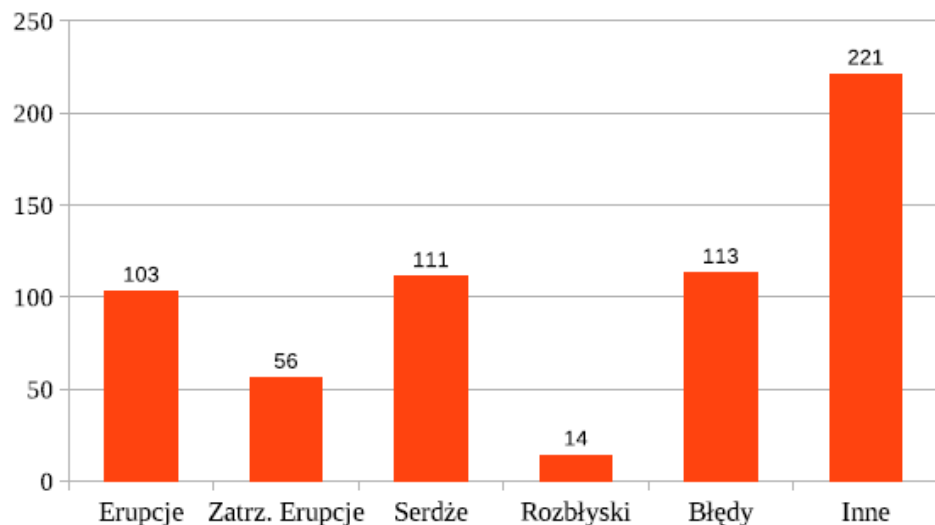
Eruption

30-May-12
01:46:13.340
02:48:13.340
03:00:13.340

center (x,y) -1045, 40
frames: 38



Results

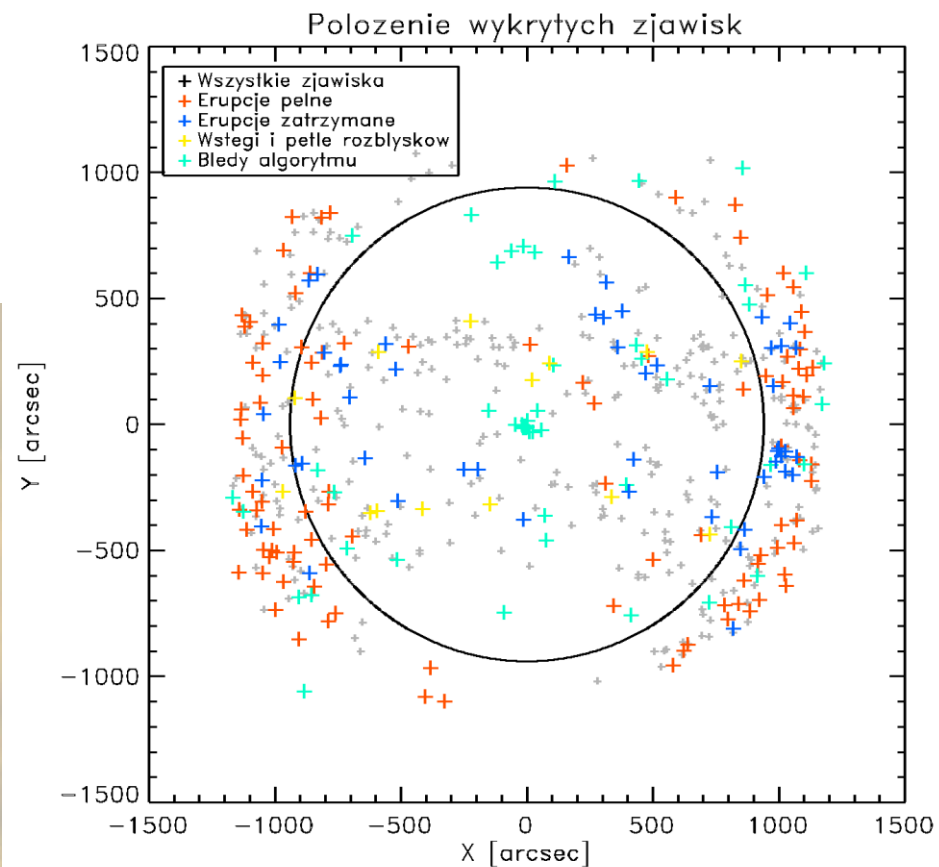


1 APR 2012 – 1 JUL 2012

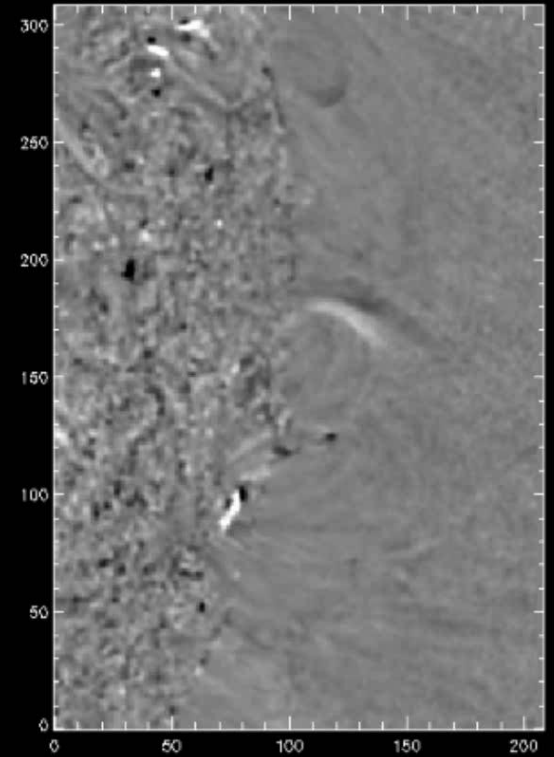
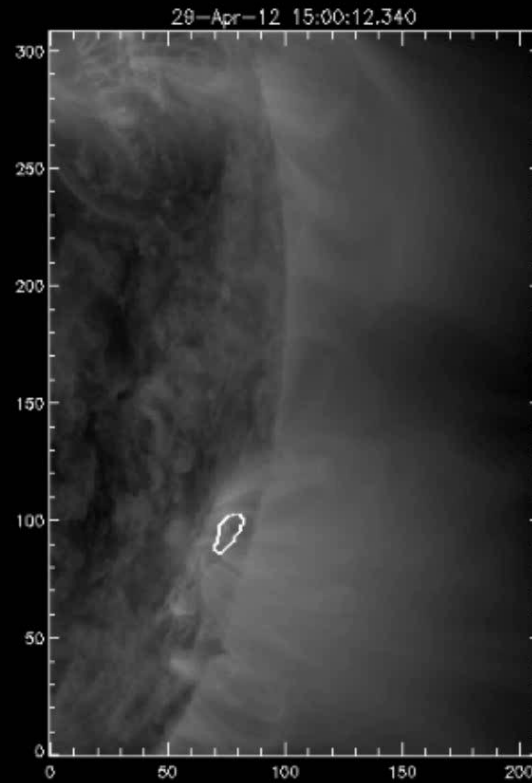
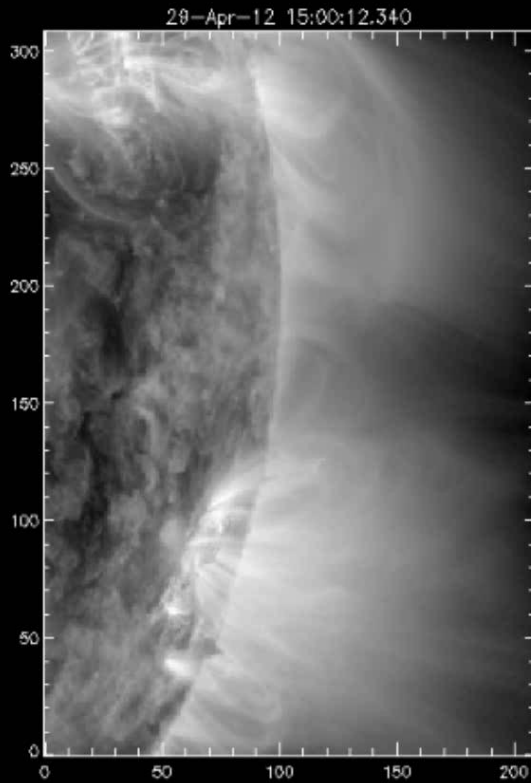
618 moving features recognized

Half of them were eruptions, surges, and flares

Classification was made by user. We did not use automatic feature recognition.



Automatic height profile.

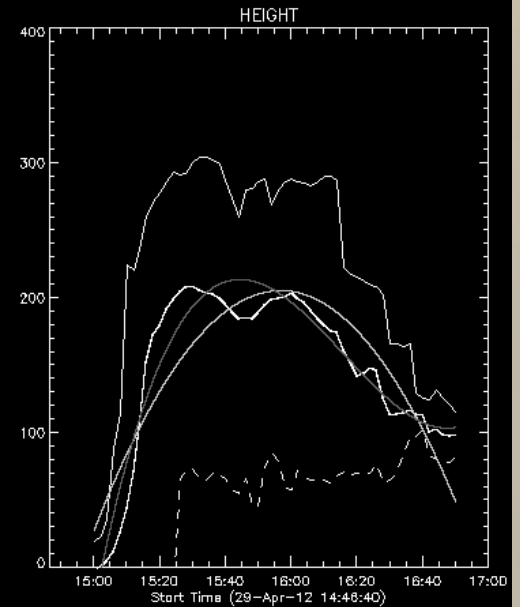
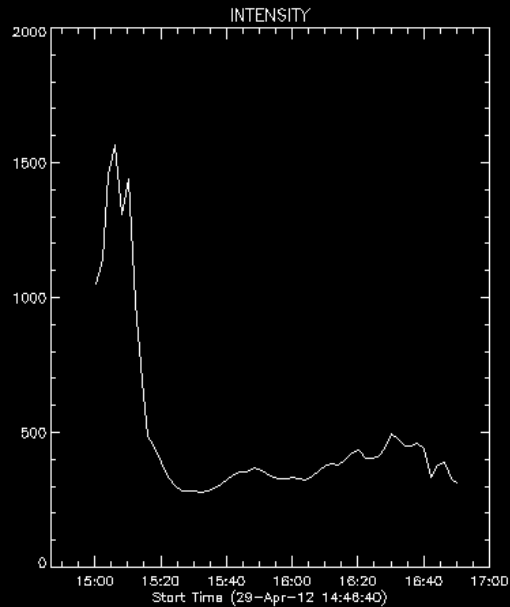
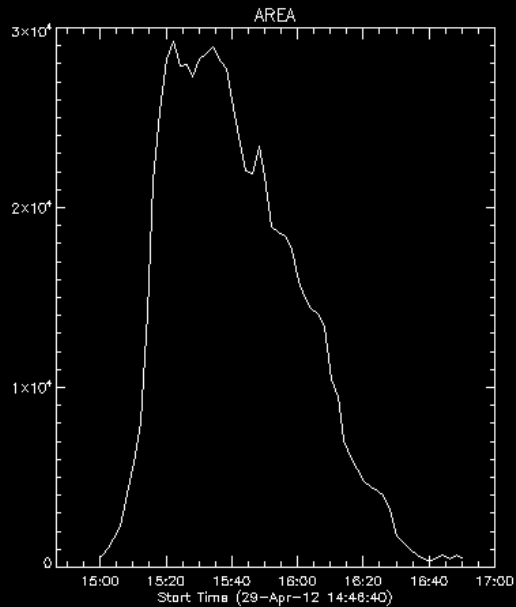
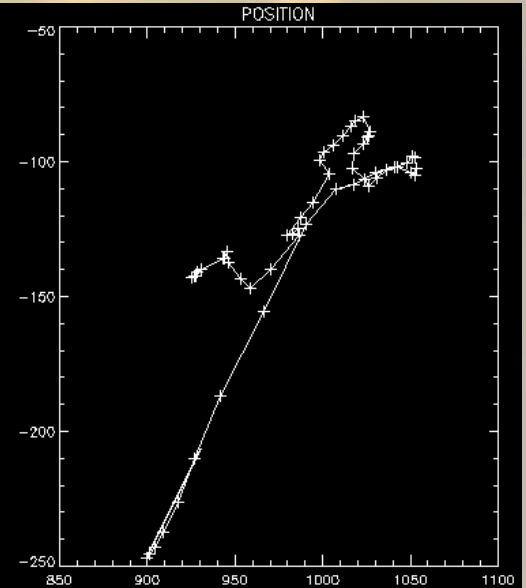
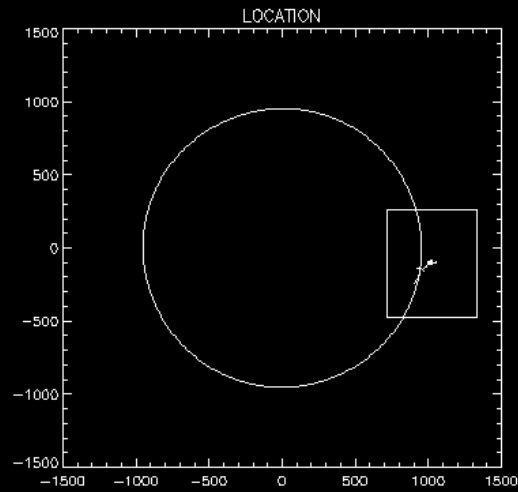


Automatic height profile.

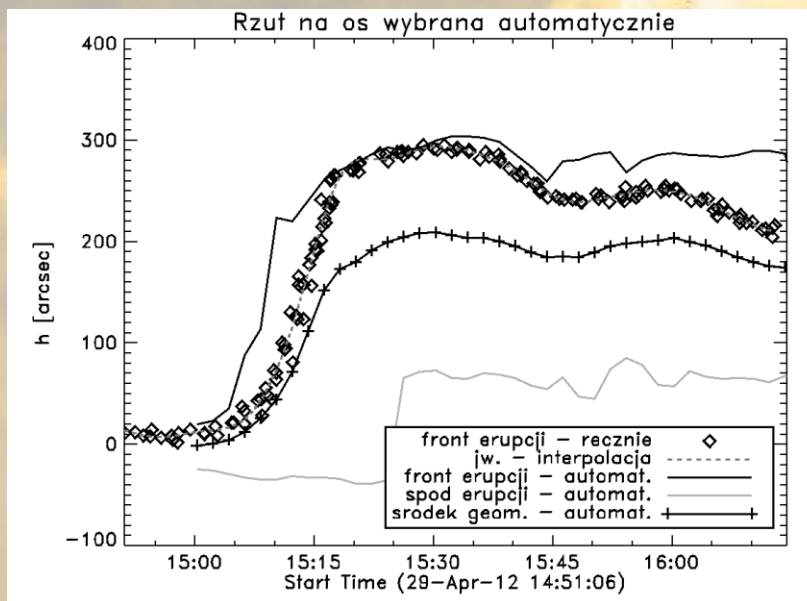
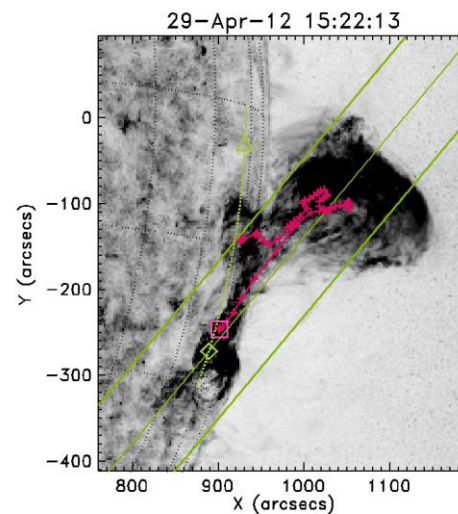
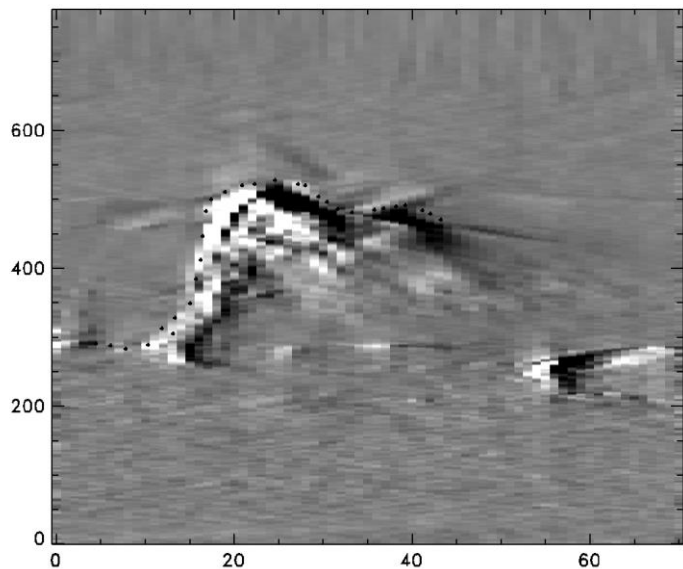
Eruption

29-Apr-12
15:00:13.340
15:22:13.340
16:50:13.340

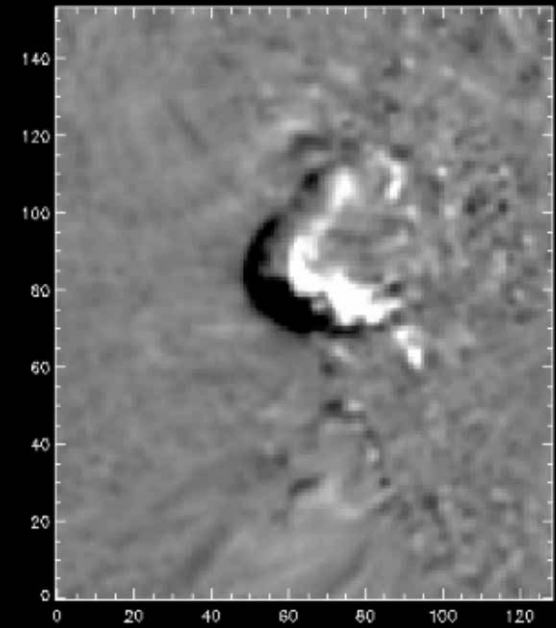
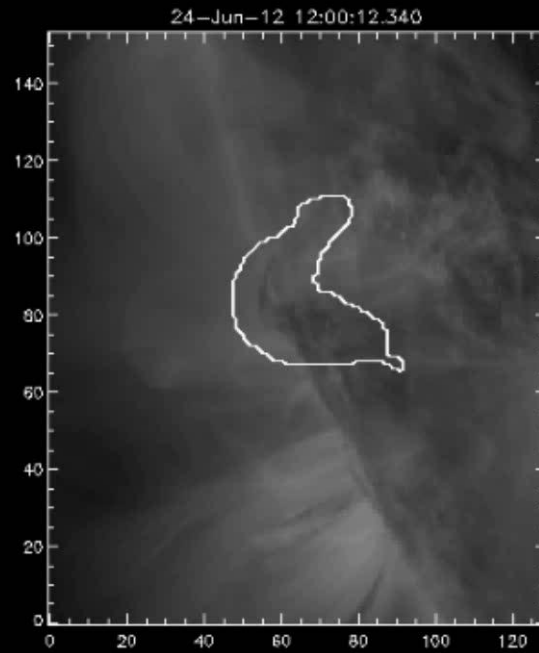
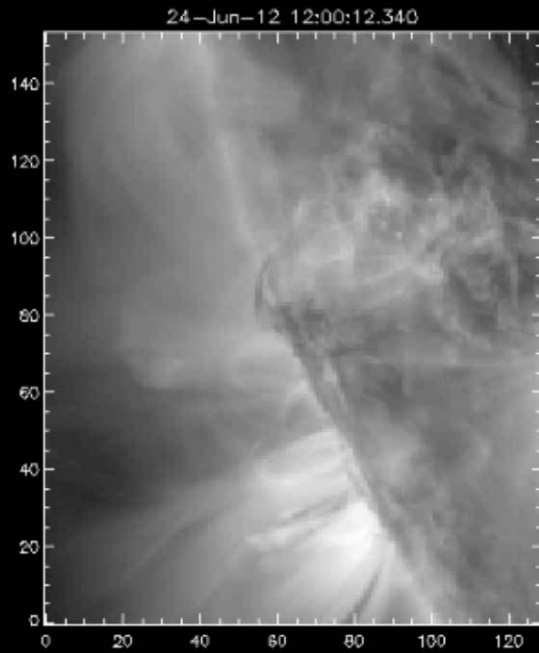
center (x,y) 1024, -106
frames: 56



Automatic height profile.



Automatic height profile. Bad case.

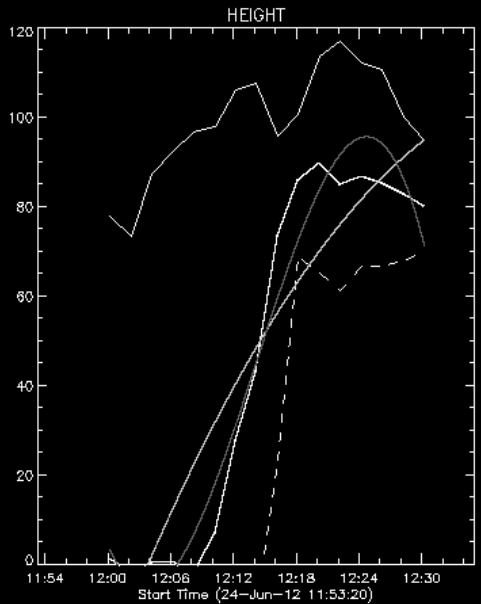
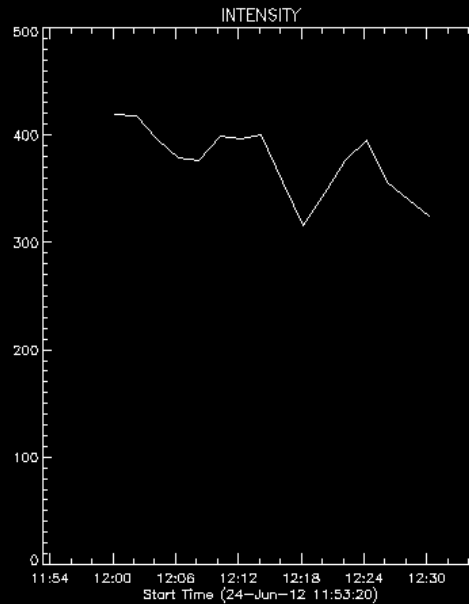
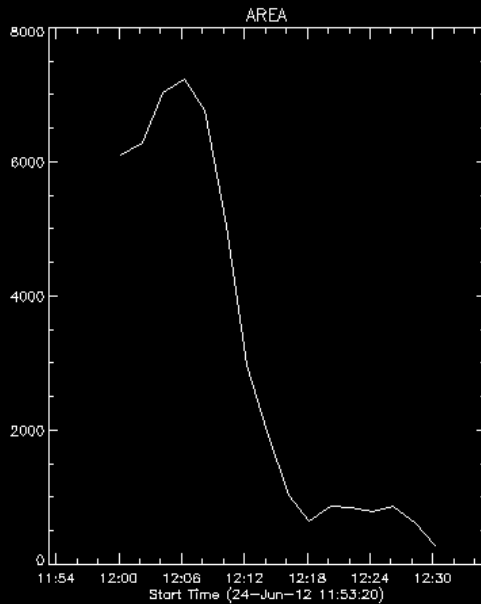
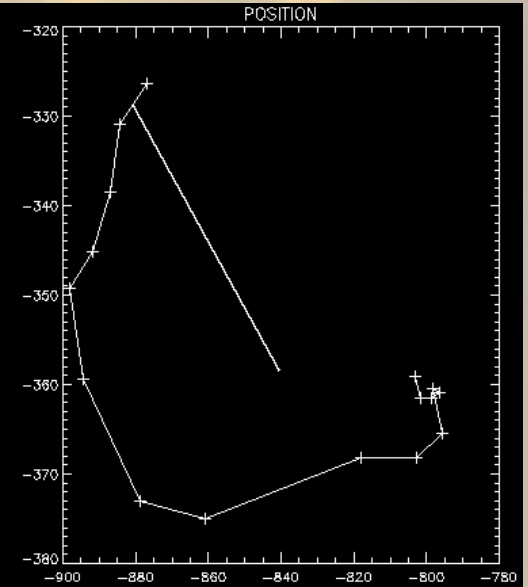
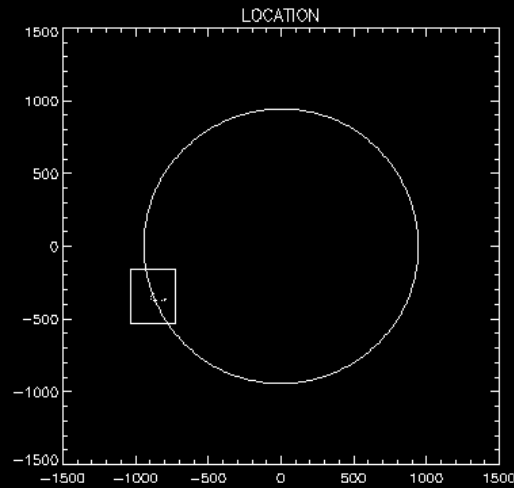


Automatic height profile. Bad case.

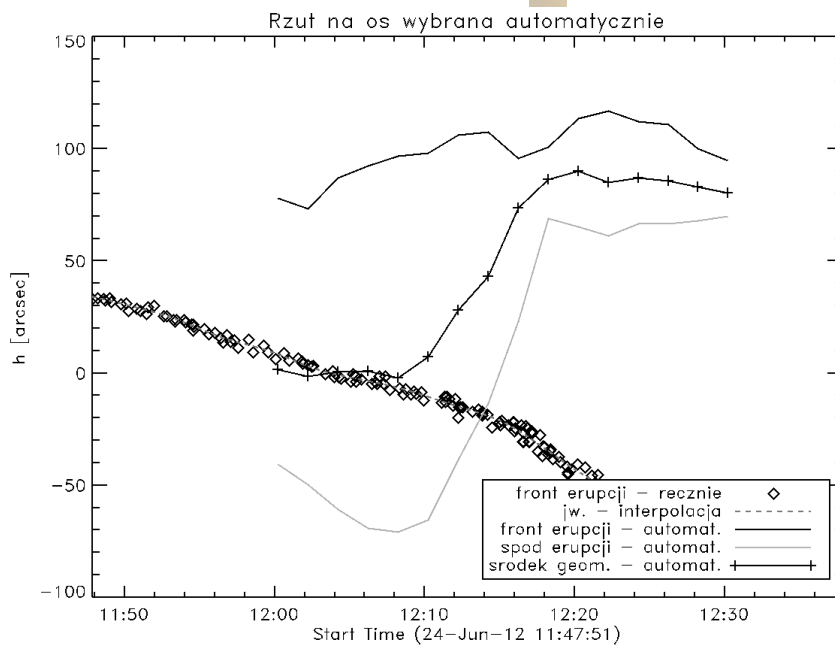
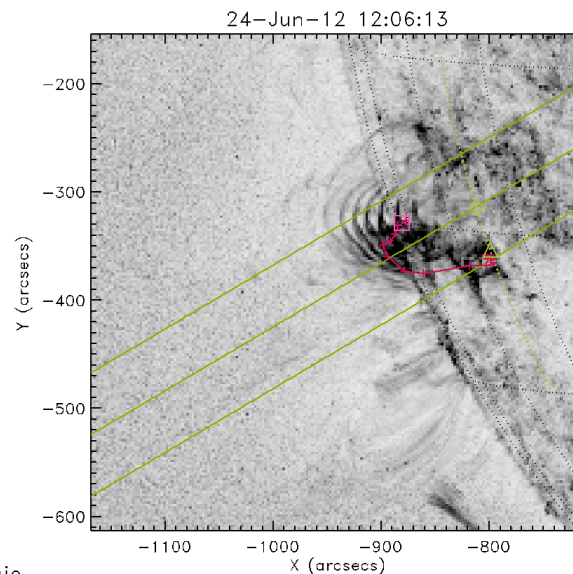
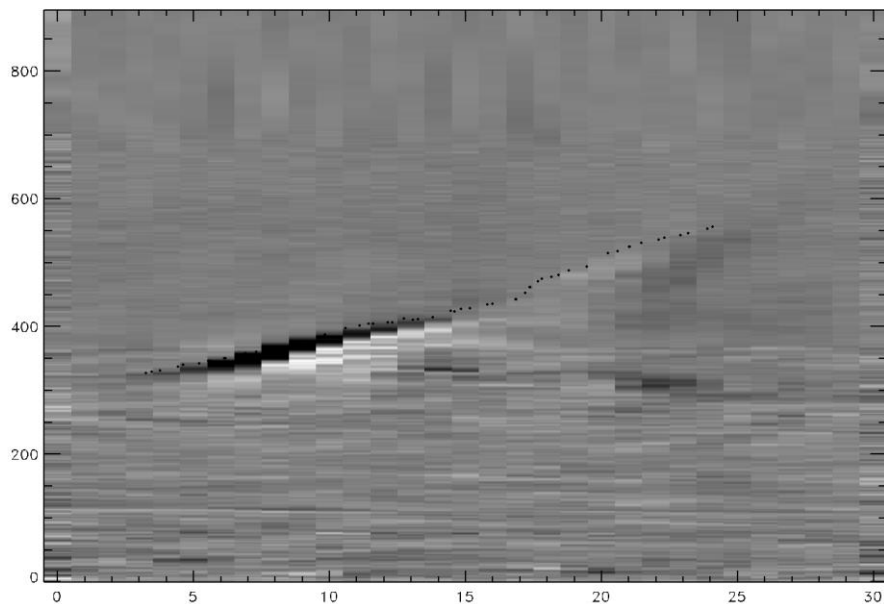
Eruption

24-Jun-12
12:00:13.340
12:06:13.340
12:30:13.340

center (x,y) -879, -345
frames: 16

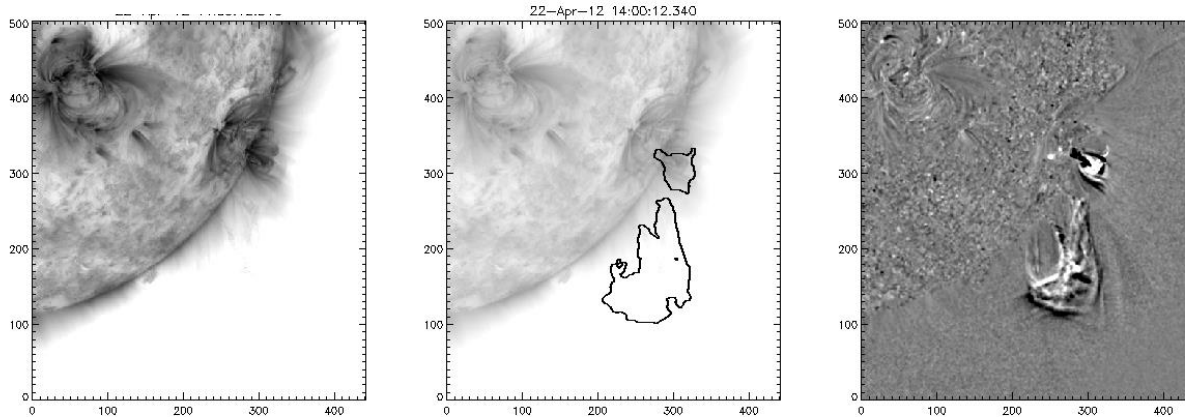


Automatic height profile. Bad case.

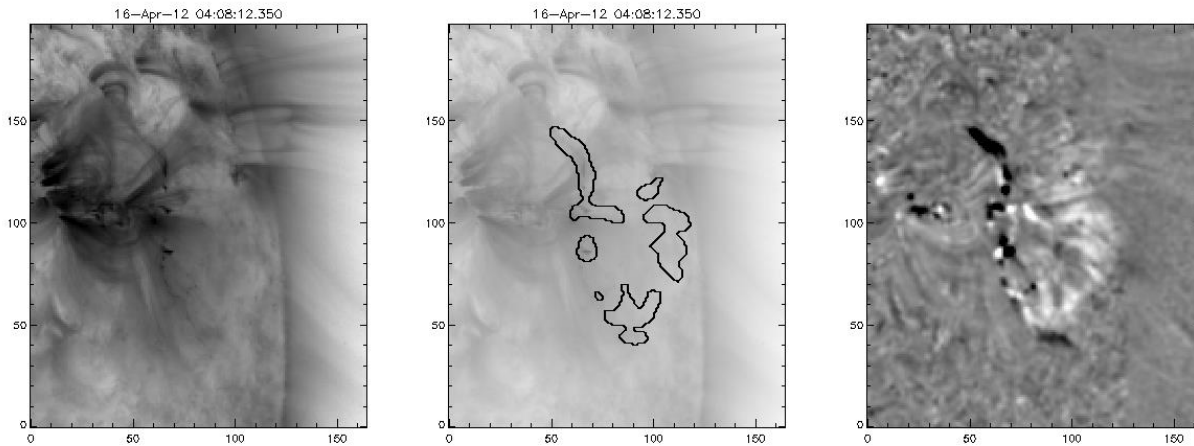


Automatic classification. Failed.

Simultaneous events



Low signal. Event lost.



Main problems with automatic classification of events:

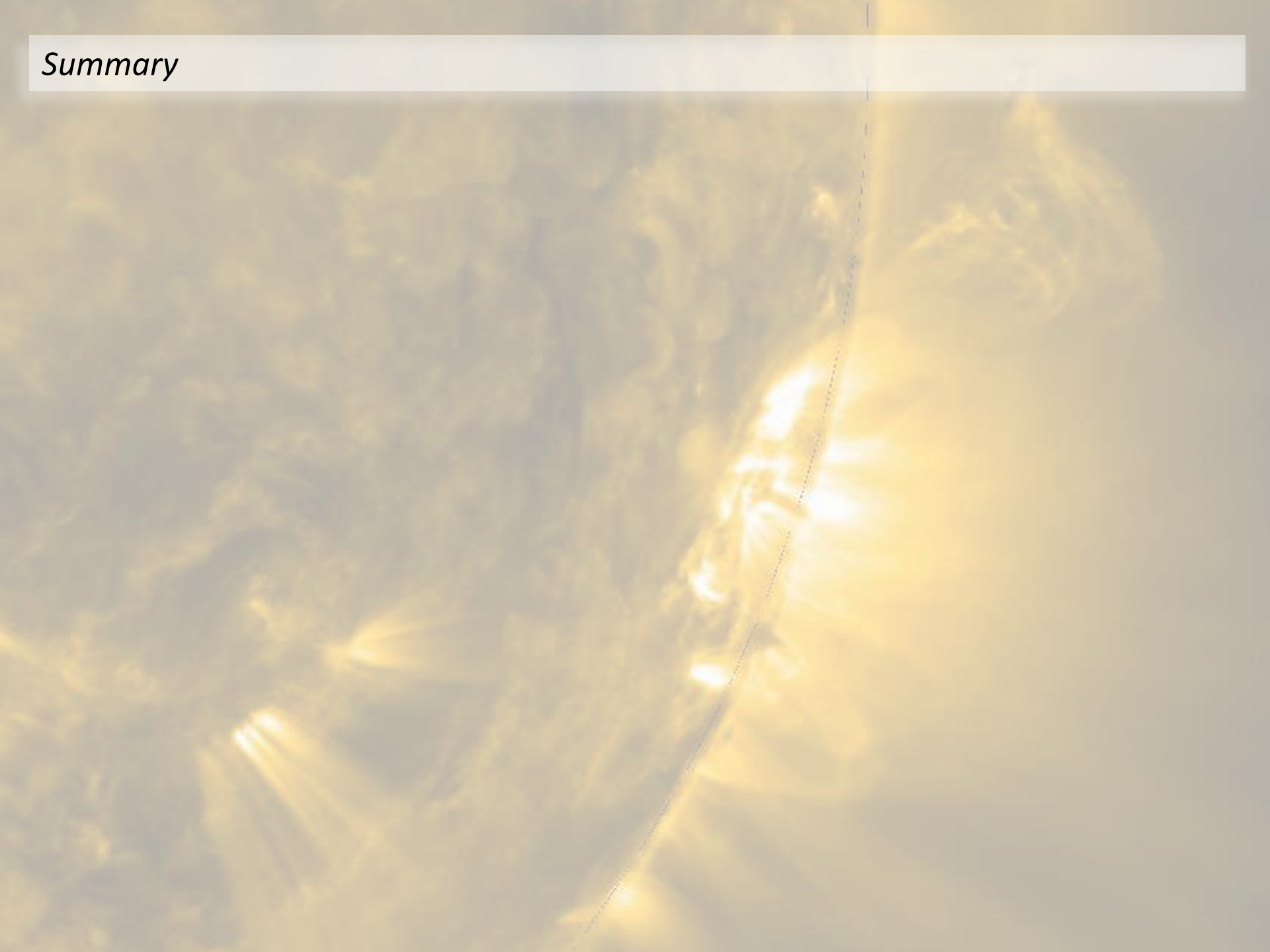
1. Detection threshold. Very important for on-disk-events.
2. Escaping from field of view – false failed eruption detection.
3. Oscillating loops.
4. Events blending.
5. Simultaneous eruptions.

The method is very effective for recognition of moving features but next steps have to be done „by hand”

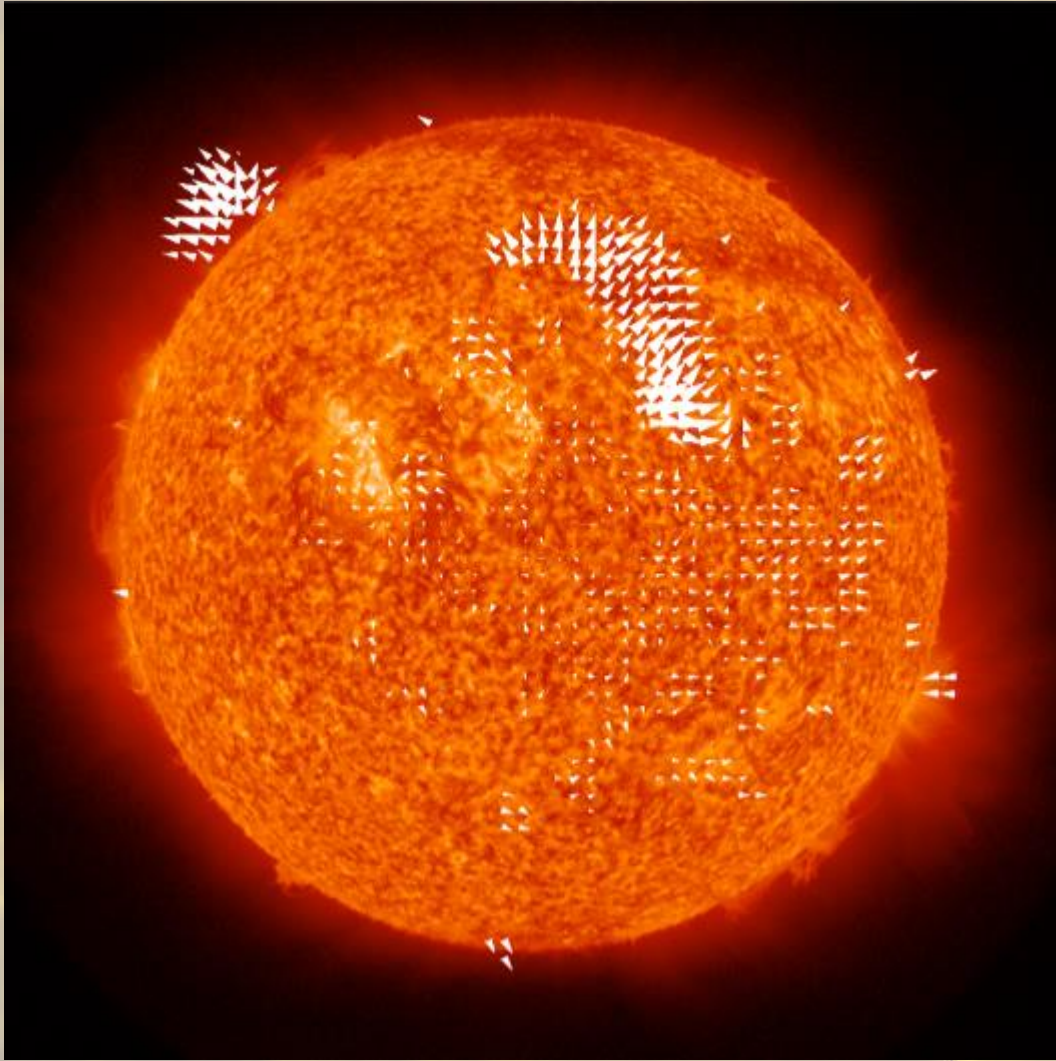
Few more remarks & summary

- New algorithm was constructed, and used for SDO/AIA 171 Å observations
- More effective than algorithm described by Hurlburt, N. 2015 (arXiv:1504.03395) and Hurlburt, N. & Jaffey, S. 2015 (arXiv:1504.04660)
- Very effective for large, diffuse structures visible on the edge of AIA's field of view.
- Algorithm is very slow (3 hours of observations are analysed in 1 hour on personal computer) due to:
 - slow data transfer, unstable connection with JSOC server
 - last step (searching for pixels with $P(E|\hat{x}) > 0.35$) was very time-consuming – growth algorithm
- Usefull for preliminary data search. Next steps – events classification, parameters – have to be done by user.

Summary



Hurlburt



Optical flow method

Problem klasyfikacji zjawisk

- **Coronal transients.** A general term for short-time-scale changes in the corona. Includes CMEs.
- **Active dark filament (ADF).** A filament displaying motion or changes in shape, location, or absorption characteristics.
- **Active prominence.** A prominence above the solar limb moving and changing in appearance over a few minutes of time.
- **Bright surge on the disk (BSD).** A bright stream of gas seen against the solar disk. BSDs are often flare related and commonly fan out from the flare site.
- **Bright surge on the limb (BSL).** A bright stream of gas emanating from the chromosphere that moves outward more than 0.15 solar radius above the limb. It may decelerate and return to the Sun. Most BSLs assume a linear radial shape but can be inclined and/or fan shaped.
- **Dark surge on the disk (DSD).** Dark gaseous ejections on the Sun visible in Ha. They usually originate from small subflare-like brightenings. Material is usually seen to be ejected, then decelerate at a gravitational rate, and to flow back to the point of origin. DSDs can occur intermittently for days from an active region.
- **Disappearing solar filament (DSF).** A solar filament that disappears suddenly on a timescale of minutes to hours. The prominence material is often seen to ascend but can fall into the Sun or just fade. DSFs are probable indicators of coronal mass ejections.
- **Eruptive prominence on limb (EPL).** A solar prominence that becomes activated and is seen to ascend away from the Sun; sometimes associated with a coronal mass ejection.
- **Spray (SPY).** Luminous material ejected from a solar flare with sufficient velocity to escape the Sun (675 km/s). Sprays are usually seen in H-alpha with complex and rapidly changing form. There is little evidence that sprays are focused by magnetic fields.
- **Surge.** A jet of material from active regions that reaches coronal heights and then either fades or returns into the chromosphere along the trajectory of ascent. Surges typically last 10 to 20 minutes and tend to recur at a rate of approximately 1 per hour. Surges are linear and collimated in form, as if highly directed by magnetic fields.